Selective activation of adrenoceptors potentiates I_{Ks} current in pulmonary vein cardiomyocytes through the protein kinase A and C signaling pathways

Xinya Mi[1], Wei-Guang Ding[1] M.D., Ph.D., Futoshi Toyada[1] Ph.D., Akiko Kojima[2] M.D., Ph.D., Mariko Omatsu-Kanbe[1] Ph.D. and Hiroshi Matsuura[1] M.D., Ph.D.

Department of [1]Physiology and [2]Anesthesiology, Shiga University of Medical Science, Otsu, Shiga, Japan

Correspondence author

Wei-Guang Ding, M.D., Ph.D.

Department of Physiology

Shiga University of Medical Science,

Otsu, Shiga 520-2192, Japan

Tel: 81-77-548-2152

Fax: 81-77-548-2348

E-mail: ding@belle.shiga-med.ac.jp

Abstract

Delayed rectifier K^+ current (I_{Ks}) is a key contributor to repolarization of action potentials. This study investigated the mechanisms underlying the adrenoceptor-induced potentiation of I_{Ks} in pulmonary vein cardiomyocytes (PVC). PVC were isolated from guinea pig pulmonary vein. The action potentials and I_{Ks} current were recorded using perforated and conventional whole-cell patch-clamp techniques. The expression of I_{Ks} was examined using immunocytochemistry and Western blotting. *KCNQ1*, a I_{Ks} pore-forming protein was detected as a signal band approximately 100 kDa in size, and its immunofluorescence signal was found to be mainly localized on the cell membrane. The I_{Ks} current in PVC was markedly enhanced by both β_1- and β_2-adrenoceptor stimulation with a negative voltage shift in the current activation, although the potentiation was more effectively induced by β_2-adrenoceptor stimulation than β_1-adrenoceptor stimulation. Both β-adrenoceptor-mediated increases in I_{Ks} were attenuated by treatment with the adenylyl cyclase (AC) inhibitor or protein kinase A (PKA) inhibitor. Furthermore, the I_{Ks} current was increased by α_1-adrenoceptor agonist but attenuated by the protein kinase C (PKC) inhibitor. PVC exhibited action potentials in normal Tyrode solution which was slightly reduced by HMR-1556 a selective I_{Ks} blocker. However, HMR-1556 markedly reduced the β-adrenoceptor-potentiated firing rate. The stimulatory

effects of β- and α_1-adrenoceptor on I_{Ks} in PVC are mediated via the PKA and PKC signal pathways. HMR-1556 effectively reduced the firing rate under β-adrenoceptor activation, suggesting that the functional role of I_{Ks} might increase during sympathetic excitation under *in vivo* conditions.

Keywords

Pulmonary vein cardiomyocytes, Adrenocptors, I_{Ks}, AC-cAMP-PKA pathway, PKC pathway

Abbreviations

AF atrial fibrillation

PVs pulmonary veins

PVC pulmonary vein cardiomyocytes

SA sinoatrial

LA left atrial

LV left ventricular

I_{Ks} the slow component of delayed rectifier K^+ current

I_{Kr} the fast component of delayed rectifier K^+ channel

I_{K1} the inwardly rectifying K^+ current

I_f the hyperpolarization-activated cation current

G_s stimulatory G protein

G_i inhibitory G protein

AC adenylyl cyclase

PKA protein kinase A

PKC protein kinase C

BIS-I bisindolylmaleimide

DMSO dimethylsulfoxide

DAPI 4′-6′-diamidino-2-phenylindole

PBS phosphate-buffered saline

TBST Tris-buffered saline with 0.1% Tween-20

1. Introduction

Atrial fibrillation (AF) is the most common of all sustained cardiac arrhythmias in humans, manifesting more frequently with age and being typically caused by stroke, although the mechanisms underlying the initiation of AF are still not fully understood [1]. Early studies reported that the walls of pulmonary veins (PVs) have a myocardial muscle layer connected to left atrial cardiac myocytes, which generate spontaneous automaticity (action potentials) [2]. This automaticity can be enhanced and propagated into the left atrium by treatment with digitalis toxicity [3]. Of note, paroxysmal AF in humans is initiated by ectopic beats originating from the PVs [4]. Many subsequent clinical and experimental studies confirmed that PVs are important sources of ectopic beats for the initiation of paroxysmal and chronic AF [5, 6]. Furthermore, a reduction in the PVs focus through ablation is effective for treating acute and sustained AF, suggesting dynamic interaction between the left atrial (LA) and PVs ectopic activity [7, 8].

The basic electrophysiological and pharmacological properties of PVs and pulmonary vein cardiomyocytes (PVC) have been reported in various experimental species, including dogs [9], rabbits [10], rats [11, 12] and guinea pigs [2, 13, 14]. The electrical properties of PVs were reported to differ markedly from the left atrium, and their ectopic automaticity

might also be induced via different mechanisms from the sinus node [5, 6]. Previous studies have reported that PVC favor the occurrence of reentry due to shorter action potentials, apparently due to a lower voltage-dependent L-type Ca^{2+} current [15, 16]. In addition, PVC have a lower negative resting membrane potential than the left atrium due to the lower density of the inwardly rectifying K^+ current (I_{K1}) in canine [16] and guinea pig models [13]. A recent study reported that the electrical activity of rat PVC is suppressed by treatment with inhibitors of sarcoplasmic reticulum and membrane Na^+/Ca^{2+} exchanger, and similar results were confirmed in other experimental species [17]. These results suggest that the increases in intracellular Ca^{2+} induced by the sarcoplasmic reticulum and the enhanced activity of the Na^+/Ca^{2+} exchanger might influence the ectopic automaticity of PVs.

The slow component of the delayed rectifier K^+ channel (I_{Ks}) has been shown to exist in the cardiac myocytes of various mammalian species, including humans [18]. The I_{Ks} channel is formed by two subunits: *KCNQ1* (pore-forming α-subunit) and *KCNE1* (β-subunit) [19, 20]. In human and guinea pigs, I_{Ks} is activated slowly following the upstroke of the action potential and has an important role in providing an outward current to initiate the phase 3 repolarization of atrial and ventricular action potentials [21, 22]. Furthermore, a previous report showed that, in sinoatrial (SA) node cells, the deactivation process of the

delayed rectifier K^+ current at the repolarizing phase plays a crucial role in providing diastolic depolarization [23]. We previously reported that suppression of the I_{Ks} current by its selective blocker delays the repolarization process and markedly reduces the pacemaker activity in SA node cells of guinea pigs [24, 25] suggesting that I_{Ks} can contribute to the repolarizing process in SA node cells, which is important for determining the pacemaker activity. Of note, in the presence of β-adrenergic stimulation condition the dominance contribution involved in the cardiac action potential shifted from the delayed rectifier K^+ channel (I_{Kr}) to I_{Ks} [26], so I_{Ks} may regulate cardiac excitement and contraction by various extracellular signaling molecules. Indeed, we and other groups have shown that β-adrenergic stimulation preferentially enhances I_{Ks} in guinea pig ventricular myocytes [27, 28], SA node cells [29] and human atrial myocytes [30]. We suspect that, during sympathetic or exercised stimulation, both Ca^{2+} and the I_{Ks} current are enhanced, so potentiated I_{Ks} may maintain a proper balance between the inward and outward currents, thereby regulating cardiac pacemaker activity and contraction.

Given these previous findings, we hypothesized that adrenergic signal activation might regulate the function of I_{Ks} in PVC, and I_{Ks} might modify the property of PVC automaticity, especially under adrenoceptor-stimulated conditions. We therefore investigated

1) whether or not I_{Ks} is functionally present in guinea pig PVC and 2) whether or not its activity and contribution to the automaticity are modulated during sympathetic excitation. Since the adrenergic signal pathway regulates the heart function through different receptor subtypes [31, 32], the present study investigated the electrophysiological properties of I_{Ks} and compared the effects of β_1-, β_2- and α_1-adrenergic receptor stimulation on I_{Ks} in PVC.

2. Materials and methods

2.1 Preparations

All animal care and experimental procedures were conducted in accordance with the *Guide for the Care and Use of Laboratory Animals* published by the US National Institutes of Health (NIH Publication No. 85-23, revised 1996) and were approved by the institution's Animal Care and Use Committee of Shiga University of Medical Science (approval number, 2018-7-3). Female Hartley guinea pigs (4-6 weeks old, 250-400 g) were used in the present experiments. The studies involving animals were reported in accordance with the ARRIVE guidelines for reporting experiments involving animals [33].

PVC and LA preparations were isolated using an enzymatic dispersion procedure similar to that described previously [2, 13, 25]. In brief, the heart and lung lobes were promptly removed from the open chest of guinea pigs deeply anaesthetized with sodium pentobarbital (intraperitoneal [i.p.], 120 $mg \cdot kg^{-1}$). The ascending aorta was cannulated *in situ*, while the heart and lobes were excised and retrogradely perfused via the aortic cannula on a Langendorff apparatus at 37 °C initially for 4 min with normal Tyrode solution and then for 4 min with nominally Ca^{2+}-free Tyrode solution. All of these solutions were oxygenated with 100% O_2. This was followed by 8-10 min of perfusion with nominally Ca^{2+}-free Tyrode

solution containing 0.4 $mg \cdot mL^{-1}$ collagenase (Wako Pure Chemical Industries, Osaka, Japan). The left atrium was dissected from the heart, chopped into small pieces, and subsequently dispersed into single cells. The four digested tubular PVs were dissected from the LA-PVs junction and then chopped into small strips. The strips were further digested at 37 °C for 40 min with solution containing 1.0 $mg \cdot mL^{-1}$ collagenase and 0.1 $mg \cdot mL^{-1}$ elastase (Wako Pure Chemical Industries). Finally, the PV strips were gently agitated in a high-K^+, low-Cl^- KB solution, and isolated PVC and LA cells were stored at 4 °C in the KB solution for experimental use within 8 h.

2.2 Solutions and chemicals

Normal Tyrode solution contained (in mM) 140 NaCl, 5.4 KCl, 1.8 $CaCl_2$, 0.5 $MgCl_2$, 0.33 NaH_2PO_4, 5.5 glucose and 5 HEPES (pH adjusted to 7.4 with NaOH). KB solution contained (in mM) 70 K-glutamate, 30 KCl, 10 KH_2PO_4, 1 $MgCl_2$, 20 taurine, 0.3 EGTA, 10 glucose and 10 HEPES (pH adjusted to 7.2 with KOH). The pipette solution contained (in mM) 70 potassium aspartate, 70 KOH, 50 KCl, 10 KH2PO4, 1 $MgSO_4$, 3 Na_2-ATP (Sigma Chemical Company, St Louis, MO, USA), 5 EGTA, 5 HEPES, 0.1 Li_2-GTP (Sigma Chemical Company) and 2 $CaCl_2$ (pH adjusted to 7.2 with KOH). Norepinephrine (Sigma Chemical

Company), isoproterenol (Sigma Chemical Company) and phenylephrine (Sigma Chemical Company) were dissolved in distilled water as 10-mM, 1-mM and 30-mM stock solution, respectively. Nisoldipine (Sigma Chemical Company) was prepared as a 1-mM stock solution in ethanol and then diluted in the external solution to achieve a concentration of 0.4 μM. E4031 (Wako Pure Chemical Industries) was dissolved in distilled water as a 5-mM stock solution. CGP 20712A (Sigma Chemical Company) was dissolved in distilled water as a 1-mM stock solution. HMR-1556 (a generous gift from Hoechst Marion Roussel, Frankfurt, Germany) was dissolved in dimethylsulfoxide (DMSO) as a 10-mM stock solution. Stock solutions were made in DMSO (bisindolylmaleimide I [BIS-I], 1 mM, Sigma Chemical Company; ICI 118551, 1 mM, Sigma Chemical Company; denopamine, 1 mM, Santa Cruz Biotechnology, Inc., Dallas, TX, USA; zinterol, 2 mM, Sigma Chemical Company; H89, 20 mM, Sigma Chemical Company; SQ 22536, 300 mM, Enzo Life Sciences, Inc., Farmingdale NY, USA; prazosin, 10 mM, Sigma Chemical Company). The experimental concentration of DMSO and ethanol was less than 0.1%, and the concentrations of solvents had no influence on the membrane ion currents.

2.3 Whole-cell patch-clamp recording

Perforated and conventional (ruptured) whole-cell patch-clamp techniques were used to record the action potentials and membrane currents from PVC in the current- and voltage-clamp modes, respectively, with an EPC-8 patch-clamp amplifier (HEKA, Lambrecht, Germany), as previously described [24, 25]. The patch electrodes had a resistance of 2.0-4.0 MΩ when filled with the pipette solution. PVC were transferred to a 0.5-ml chamber and were perfused with extracellular solution at 35-37 °C. PVC were confirmed by action potentials in normal Tyrode solution. I_{Ks} current was elicited by depolarizing pulses delivered from a holding potential of –50 mV (Na^+ current was inactivated by setting the holding potential) to various levels under conditions where $I_{Ca,L}$ and I_{Kr} were blocked by nisoldipine (0.4 μM) and E-4031 (5 μM), respectively [25]. The electrical activity of I_{Ks} was evaluated by measuring the amplitude of the tail current elicited upon repolarization to the holding potential. Activation of β_1-adrenoceptor was conducted with the β_1-agonist denopamine [34] in the presence of the β_2-adrenoceptor antagonist ICI 118551 [35, 36]; activation of β_2-adrenoceptor was conducted with the β_2-agonist zinterol in the presence of the β_1-adrenoceptor antagonist CGP 20712A [35, 36]. For action potential recording, amphotericin B (100 $\mu g \cdot mL^{-1}$; Wako Pure Chemical Industries) was added to the pipette solution.

The voltage dependence of I_{Ks} activation was evaluated by fitting the amplitude of the normalized tail current ($I_{Ks,tail}$) to a Boltzmann equation:

$$I_{Ks,tail} = 1 / \{1 + \exp[(V_{1/2} - V_t) / k]\},$$

where $V_{1/2}$ is the voltage at half-maximal activation, V_t is the test potential, and k is the slope factor. The cell membrane capacitance (C_m) was calculated for each cell from the capacitive current elicited by 20-ms voltage-clamp steps (±5 mV) according to the following equation:

$$C_m = \tau_C I_0 / \Delta V_m (1 - I_\infty / I_0),$$

where τ_C is the time constant of the capacitive current, I_0 is the initial peak current amplitude, I_∞ is the steady-state current value, and ΔV_m is the amplitude of the voltage step [37]. The calculated cell sizes of PVC and the LA and left ventricular (LV) were 77.38 ± 4.93 pF (n = 60, N = 15), 45.98 ± 4.07 pF (n = 15, N = 6) and 106.80 ± 7.31 pF (n = 15, N = 6), respectively.

2.4 Immunocytochemistry

The procedure was performed with reference to a previous report [38]. Appropriate concentrations of PVC were immobilized on glass-bottom dishes pre-coated with the

biological glue Cell-Tak (Corning, Inc., NY, USA) without overlap and then incubated for 40 min at room temperature. The cells were incubated with cell membrane staining kit working solution (AAT Bioquest Inc., CA, USA) at 37°C for 20 min and protected from light, then rinsed with phosphate-buffered saline (PBS) and fixed with 4% paraformaldehyde (Nacalai tesque, Kyoto, Japan) for 20 min with shaking. After washing the fixed cells with PBS for 10 min three times, they were incubated for 60 min at room temperature in blocking-permeabilization solution. The cells were incubated with *KCNQ1* antibody (1:300 dilution in blocking-permeabilization solution; Merck Millipore, Darmstadt, Germany) for 60 min, and then with the secondary antibody AlexaFluor anti-rabbit 488 nm IgG (1:400 dilution in the blocking solution; Molecular Probes, Thermo Fisher Scientific, MA, UK) for 120 min at room temperature. After washing the cells, the nuclei were stained with 4′-6′-diamidino-2-phenylindole (DAPI) (1:10000 dilution; Merck Millipore). The fluorescent signals were assessed using a Leica TCS SP8 LIGHTNING confocal microscope (Wetzlar, Germany).

2.5 Western blotting

The procedure was performed with reference to a previous report [38]. Pulmonary vein

sleeves were lysed in Tris buffer supplemented with protease inhibitor (Complete Mini; Mannheim, Germany), homogenized and then incubated on ice for 40 min before being centrifuged at 15,000 rpm for 20 min. The amount of protein was quantified using a protein assay (Bio-Rad, Richmond, CA, USA), diluted to its final concentration using 1x Sample buffer solution (FUJIFILM, Tokyo, Japan) and 2% 2′ mercaptoethanol and then denatured for 60 min at 37 °C. In the present study, lysate containing protein (5 μg per lane) was separated on a 5%-20% sodium dodecyl sulfate-polyacrylamide gel (Wako Pure Chemical Industries), and proteins were then electrotransferred to a polyvinylidene difluoride membrane (Merck Millipore). The transferred membrane was blocked with 5% skim milk (Nacalai Tesque) diluted in Tris-buffered saline with 0.1% Tween-20 (TBST) for 60 min at room temperature. The membrane was probed with *KCNQ1* AB5932 antibody (1:500 dilution in TBST; Merck Millipore) and anti-glyceraldehyde 3-phosphate dehydrogenase (GAPDH) (Cell Signaling Technology, Danvers, MA, USA) overnight at 4 °C. After being washed 5 times with TBST, the membrane was incubated with anti-rabbit IgG antibody (1:10000 dilution in TBST; GE Healthcare Bio-Sciences KK, Tokyo, Japan) for 120 min at room temperature. After the membrane was washed, immunosignals were detected with a chemi-luminescence one ultra assay (Nacalai Tesque) and analyzed using a lumino-image analyzer (FUJIFILM).

2.6 Statistical analyses

All of the average data were presented as the mean ± standard error of the mean. Statistical comparisons were evaluated using an analysis of variance with Student's unpaired t-test or using a one-way analysis of variance, followed by Tukey's *post hoc* test (Prism Version 5.0), as appropriate. N indicates the number of guinea pigs and n indicates the number of cells used in experiments. Differences were considered to be statistically significant at $P < 0.05$.

3. Results

3.1 The expression, localization and current density of I_{Ks} in PVC and LA

The protein expression of *KCNQ1* (pore-forming α-subunit of I_{Ks} channel) of PVC and LA was examined as shown in Figure 1A, the positive single band of *KCNQ1* of roughly 100 kDa was detected by Western blotting, as previously reported in mouse cardiomyocytes [39] and human iPS Cell-Derived cardiomyocytes [40]. The positive single band of *KCNE1* (pore-forming β-subunit of I_{Ks} channel) was detected approximately 17 kDa in size (Supplementary material 1), supported by the previous results obtained in rat heart [41]. The current density of I_{Ks} in PVC and LA was 3.1 ± 0.24 pA/pF and 1.65 ± 0.40 pA/pF, respectively (Figure 1B). In addition, our investigation using immunochemical staining and three-dimensional images shows that the I_{Ks} (*KCNQ1*), positive signal was mainly colocalized with membrane marker on the surface of PVC and LA myocytes (Figure 1C), indicating its functional role as an ion channel.

3.2 Involvement of the β-adrenoceptor and relevant signaling pathway in I_{Ks} potentiation

To determine the ionic basis of I_{Ks} in PVC for β-adrenergic stimulation, we examined the effects of sympathetic stimulation on I_{Ks} current by applying a physiological isoproterenol

(nonselective β-agonist, 0.1 μM) and neurotransmitter norepinephrine (adrenoceptor agonist, 5 μM). Figure 2 shows a representative experiment examining the effect of isoproterenol and norepinephrine on I_{Ks} activation in PVC. As previously reported in the protocol for I_{Ks} measurement in cardiac myocytes [24], I_{Ks} was repetitively (15 s) activated by 2-s depolarizing steps of -40 mV to +40 mV applied from a holding potential of -50 mV. Isoproterenol and norepinephrine rapidly and markedly increased the amplitude of I_{Ks} current (Figure 2A, B, D, E). The potentiation of isoproterenol and norepinephrine on I_{Ks} was assessed by measuring the amplitude of the normalized tail current, which reflects the degree of I_{Ks} activation at the preceding depolarizing test potential. The voltage dependence of I_{Ks} activation was evaluated by fitting the amplitude of the normalized tail current to a Boltzmann equation, and the voltage dependence of I_{Ks} activation in the presence of isoproterenol or norepinephrine exhibited a significant negative shift (Figure 2C, F). The rates of increase in I_{Ks} by isoproterenol and norepinephrine were 158.30% ± 11.96% and 203.50% ± 18.56%, respectively (Figure 2G). Figure 2H illustrates the negative changes of $V_{1/2}$ which were recorded in the presence of isoproterenol and norepinephrine. To verify the modulation of I_{Ks} by β-adrenoceptor activation, we examined the effect of norepinephrine in the presence of prazosin (selective α_1-adrenoceptor antagonist, 2 μM). As shown in

Supplementary material 2, norepinephrine markedly increased the amplitude of I_{Ks} in the presence of prazosin; the rate of increase was 133.80% ± 16.93% (Figure 2 G).

3.3 A comparison of the β_1- and β_2-adrenoceptor-mediated potentiation of I_{Ks} current

To elucidate the response of I_{Ks} in PVC to β_1- or β_2-adrenergic stimulation, we examined the effect of denopamine (β_1-agonist, 1 μM) in the presence of ICI 118551 (selective β_2-adrenoceptor inhibitor, 0.1 μM), the effect of zinterol (β_2-agonist, 1 μM) in the presence of CGP 20712A (selective β_1-adrenoceptor inhibitor, 0.3 μM) on I_{Ks} current activation, respectively. In addition, the effect of zinterol was also examined in the presence of ICI 118551. As demonstrated in Figure 3A, denopamine markedly increased the I_{Ks} current amplitude and significantly shifted the voltage dependence of I_{Ks} activation to a negative direction (Figure 3C).

Figure 4 shows the results of a comparison of the β_1- and β_2-adrenoceptor-mediated potentiation of I_{Ks} current. Similar to the effect of β_1-adrenoceptor stimulation, zinterol also strongly enhanced the I_{Ks} current amplitude (Figure 4A, B), resulting in a significant negative shift in the I_{Ks} activation voltage (Figure 4C). Moreover, the effects of zinterol (β_2-adrenoceptor-mediated effects) upon the current amplitude (Figure 4D, E) and the shift in

the channel activation voltage (Figure 4F) were almost abolished by ICI 118551, indicating that its actions were mainly mediated by a β_2-adrenoceptor. Of note, the potentiation of I_{Ks} induced by β_2-adrenoceptor stimulation was larger than that of β_1-adrenoceptor stimulation (Figure 4G), although there was no marked difference in the negative shift in the voltage dependence of I_{Ks} activation between β_1- and β_2-adrenoceptor stimulation (Figure 4H).

To clarify the signaling pathways underlying the potentiation of I_{Ks} by β_1- and β_2-adrenergic stimulation, the effects of denopamine and zinterol were examined in the presence of H89 (protein kinase A [PKA] selective inhibitor, 25 μM) or SQ 22536 (AC inhibitor, 300 μM). As demonstrated in Figure 5A and C, the increase in I_{Ks} induced by β_1-adrenergic stimulation was significantly reduced with the inhibition of the AC-associated PKA signaling pathway. Denopamine increased the amplitude of I_{Ks} current at +40 mV increased by 74.10% ± 8.16%. The rates of increase of 35.11% ± 7.67% and 39.63% ± 9.12% was observed in the presence of denopamine throughout with H89 or SQ 22536, respectively (Figure 5E). Similarly, the potentiation of I_{Ks} by β_2-adrenergic stimulation was also markedly decreased when the AC and PKA activities were inhibited (Figure 5B, D and F; 132.00% ± 22.69% increase in zinterol; 35.56% ± 12.45% increase in zinterol plus H89; 44.00% ± 8.37% increase in zinterol plus SQ 22536). Taken together, our data demonstrated that the

enhancement of I_{Ks} in PVC induced by β_1- and β_2-agonists is mediated through the AC-cAMP-PKA signaling pathway.

3.4 Involvement of the protein kinase C (PKC) pathway in the α_1-adrenoceptor-induced potentiation of I_{Ks}

To determine whether or not α_1-adrenergic stimulation potentiates I_{Ks} current in PVC, we examined the effect of phenylephrine (selective α_1-adrenoceptor agonist, 30 μM) on I_{Ks} activation (Figure 6A-C). Similar to the effect of β-adrenoceptor stimulation, phenylephrine markedly increased the I_{Ks} amplitude, although the negative shift in the I_{Ks} activation voltage was weaker than that seen with β-adrenoceptor stimulation. To elucidate the signaling pathway underlying the increase in I_{Ks} by α_1-adrenergic stimulation, we further examined the effect of phenylephrine in the presence of BIS-I (PKC selective inhibitor, 0.5 μM). As shown in Figure 6 (D, E), phenylephrine-induced I_{Ks} activation was significantly reduced by treatment with the PKC inhibitor. Phenylephrine increased the amplitude of I_{Ks} by 98.75% ± 10.42% and 25.25% ± 5.65% in the absence and presence of the PKC inhibitor, respectively.

3.5 Different contributions of individual adrenoceptors to the automaticity of PVC

To elucidate the effect of individual adrenoceptor-stimulation in PVC, we compared the effects of β_1-adrenergic, β_2-adrenergic and α_1-adrenergic stimulation on the automatic action potentials by applying norepinephrine. As illustrated in Figure 7A, the firing rate of the action potentials was markedly increased by norepinephrine (5 μM) (146.60% ± 32.28%). In Figure 7B, the norepinephrine-induced β_1-adrenergic activation (in the presence of prazosin and ICI 118551) significantly enhanced the firing rate by 93.83% ± 7.27%. In Figure 7C, the norepinephrine-induced β_2-adrenergic activation (in the presence of prazosin and CGP 20712A) also increased the firing rate by 27.83% ± 4.74%. In comparison to the modulation of β_1-adrenergic and β_2-adrenergic stimulation, as shown in Figure 7D, the norepinephrine-induced α_1-adrenergic-activation (in the presence of ICI 118551 and CGP 20712A) only slightly enhanced the firing rate by 11.83% ± 2.52%. In addition, the zinterol-induced β_2-adrenergic activation (in the presence of prazosin and CGP 20712A) significantly enhanced the firing rate (Figure 7E).

To further elucidate the contribution of individual β-adrenoceptors to the regulation of the firing rate of action potentials, we examined the action of β-adrenoceptor pharmacological agonists. The application of denopamine in the presence of prazosin and ICI 118551 (β_1-adrenergic activation) potentiated the firing rate by 128.20% ± 9.22%, which was

similar to the value (Figure 7G) gained from zinterol in the presence of prazosin and CGP 20712A (117.60% ± 9.84% increase, β_2-adrenergic activation).

3.6 Different contributions of I_{Ks} to the automaticity of PVC in the absence or presence of β-adrenergic stimulation

When single or cluster cells enzymatically dissociated from the LA-lung junction region were perfused with normal Tyrode solution, approximately 38.3% ± 2.2% of PVC showed electrical automaticity. When PVC were exposed to the non-selective β-adrenoceptor agonist isoproterenol, the number of beating cells increased to 50.9% ± 6.6%. We next examined the functional role of I_{Ks} in PVC automaticity under basal and β-adrenergic stimulation conditions using the I_{Ks} selective blocker HMR-1556. As illustrated in Figure 8A, PVC action potentials were slightly suppressed by HMR-1556 (1 μM). The firing rate of action potentials was reduced from 116 min^{-1} to 87 min^{-1}. In Figure 8B, the PVC action potentials were significantly enhanced by the application of isoproterenol (0.1 μM), and the firing rate rapidly increased to 252 min^{-1} from a baseline firing rate of 120 min^{-1}. The concomitant addition of HMR-1556 in the continuous presence of isoproterenol markedly suppressed the firing rate (from 252 min^{-1} to 144 min^{-1}). Of note, the blocking potency of I_{Ks} inhibitor was

higher under β-adrenoceptor-stimulated conditions than under basal conditions, suggesting a stronger functional role of I_{Ks} in the modulation of PVC automaticity during sympathetic tone (Figure 8C).

4. Discussion

The present study examined the electrophysiological properties of I_{Ks} and its modulation by stimulating different kinds of adrenergic receptors in guinea pig PVC. Our findings show that (1) the functional I_{Ks} channel (*KCNQ1*) was expressed and located on the cell membrane; (2) I_{Ks} amplitude was markedly enhanced with a negative shift in the voltage dependence of channel activation by both β_1- and β_2-adrenoceptor stimulation mediated via the AC-cAMP-PKA signaling pathway and also potentiated by α_1-adrenoceptor activation through the PKC signaling pathway; (3) separately from the β_2- and α_1-adrenergic pathways, norepinephrine more strongly potentiated the firing rate of PVC through the β_1-adrenergic pathway, whereas it noteworthy that the pharmacological activation of β_1- or β_2-adrenergic pathway increased the firing rate to a similar degree; (4) the automaticity of PVC was effective increased by stimulation with the β-adrenoceptor agonist isoproterenol and reduced in the presence of the I_{Ks} selective inhibitor HMR-1556; and (5) the I_{Ks} current density was significantly higher in PVC than in LA myocytes.

4.1 The expression and electrophysiological properties of I_{Ks} in PVC

In the present study, Western blotting and immunochemical staining and showed *KCNQ1*

proteins to be a single band with a molecular weight of roughly 100 kDa in size. Our electrophysiological experiments showed that the current kinetics of I_{Ks} in PVC were similar to those recorded from cardiac myocytes, although the current density was higher in PVC than LA myocytes, which is in agreement with the previous results obtained in canine PVC [9]. The higher density of I_{Ks} in PVC was speculated to be the reason for the shorter action potential duration in canine PVC than in the LA [9].

4.2 Involvement of underlying downstream pathways in the β_1-, β_2 and α_1-adrenoceptor-mediated enhancement of I_{Ks} current

The present study is the first to demonstrate that the stimulatory action of both β_1- and β_2-adrenoceptors on I_{Ks} in guinea pig PVC was mediated by the AC-cAMP-PKA signaling pathway. In the heart, both β_1- and β_2-adrenoceptors were reported to stimulate stimulatory G protein (G_s), which induces the production of cAMP. As a result, the cAMP-dependent protein kinase PKA modulates cardiac excitation, contraction and relaxation by phosphorylating various intracellular substrates [31, 32]. Concerning the effect of β_2-adrenoceptor activation on the contractive function, previous reports showed that the β_2-adrenoceptor is dominantly coupled to inhibitory G protein (G_i) in mouse [42] and rat [43]

cardiac myocytes. In contrast, as shown in the present study, the potentiation of I_{Ks} by β_2-adrenergic stimulation is markedly attenuated by the inhibition of the AC and PKA signaling pathways, suggesting that β_2-adrenoceptor activation in PVC is mainly coupled to G_s protein and associated with the cAMP-PKA downstream pathway. Our results are supported by previous investigations in human Fallot infants [44] and adult ventricle samples [45] as well as atrium [46] and canine ventricular myocytes [47], in which selective β_2-adrenoceptor activation potentiates the contractile and relaxant functions through the G_s and cAMP-PKA pathway. Our results found that the potentiation of I_{Ks} by α_1-adrenergic stimulation was markedly attenuated by the inhibition of the PKC signaling pathways, indicating that α_1-adrenoceptor activation in PVC is coupled to the G_q protein and the associated PKC downstream pathway. Of note, a previous study reported that the downregulation of the I_{Ks} channel occurred due to the PKC-induced acceleration of the channel endocytosis in a cell line [48], suggesting that the chronic stimulation of the α_1-adrenoceptor may lead to a decrease in I_{Ks} current mediated by PKC activation. Further research is required to address whether or not the chronic activation of PKC signaling pathway alters I_{Ks} activity in native cardiac cells.

However, the mechanisms underlying the increase in I_{Ks} current after β-adrenergic

stimulation have not been fully elucidated. One explanation is that the phosphorylation of the I_{Ks} channels by cAMP-dependent protein kinase produces a negative shift in the voltage dependence of the channel activation [49, 50], which was also demonstrated in the I_{Ks} channel of PVC in the present study. Furthermore, a recent study reported that PKA phosphorylation allows I_{Ks} single channels to open more often, more quickly and maintain a higher subconductance level [51].

Concerning the receptor number, β_1-adrenoceptor is commonly the predominant receptor subtype in mammalian heart, although the β_1/β_2-adrenoceptor ratio shows variation among species and is dependent on the region and developmental stage [31, 32]. For instance, the β_2-adrenoceptor rather than the β_1-adrenoceptor is rich in the caveolae membrane fraction in mouse and rat cardiac myocytes [52, 53]. Of note, under heart failure conditions, the expression of β_1-adrenoceptor is down-regulated, whereas that of β_2-adrenoceptor is preserved [54]. Selective blockade of β_1-adrenoceptor potentiates a positive inotropic effect to catecholamine mediated via the β_2-adrenoceptor in human atrial myocytes [55]. Interestingly, the present study showed for the first time that the I_{Ks} current amplitude in PVC is more effectively potentiated by β_2-adrenoceptor stimulation than by β_1-adrenoceptor stimulation. Indeed, a previous report on ventricular myocytes of Fallot infants mentioned

that β_2-adrenoceptor was almost as effective as β_1-adrenoceptor in regulating the positive inotropic and relaxant effects, although β_2-adrenoceptor comprise the smaller fraction of total β-adrenoceptors, suggesting that β_2-adrenoceptor is coupled more selectively to the G_s-AC-cAMP pathway than β_1-adrenoceptor in infant cardiac myocytes [44]. This selective coupling of β_2-adrenoceptor to the G_s-AC pathway was also observed in the human atrium [56] and ventricle [35]. Furthermore, the dominant subtype of β-adrenoceptors in the lungs is β_2-adrenoceptor, and the distribution between β_1- and β_2-adrenoceptor was shown to be around 22:78 in guinea pigs and 30:70 in humans, respectively [57]. These findings may explain the increased potentiation of I_{Ks} current in PVC induced by β_2-adrenoceptor activation.

4.3 The electrical automaticity of PVC and its functional regulations by adrenoceptors and I_{Ks} activation

Previous reports have shown that the isolated PVC from dogs and rabbits exhibited prominent automaticity [58, 59]. The 30% of the pulmonary vein tissue preparations isolated from guinea pig exhibited automatic electrical activity [13]. Among the isolated guinea pig PVC, the same group yielded 27% of cells showing electrical automaticity [11]. In the

present study, our results indicated that the PVC obtained by efficient isolation had relatively energetic electrical automaticity in normal Tyrode solution (38.33% ± 2.20%).

Recently, the potentiation of β-adrenoceptor in the automaticity of PVC and pulmonary vein tissue preparation was reported in rats [12] and guinea pigs [14]. In the present study, the amplitude of action potentials was slightly enhanced in the presence of isoproterenol, possibly due to the higher overshot and more negative resting potential. There may be several explanations for this phenomenon. Enhanced β-adrenergic stimulation markedly potentiates the activities of both inward current ($I_{Ca,L}$ and the hyperpolarization-activated cation current [I_f]) and outward current (I_{Ks}), by cAMP/PKA-mediated regulation as shown in SA node cells [60, 61]; under β-adrenoceptor stimulation, $I_{Ca,L}$ can be fully activated during the upstroke of the action potential, resulting in larger overshoot, while I_{Ks} can be expected to induce fast repolarization and a more negative resting potential (maximal diastolic potential) by providing more outward current. In addition, the Na^+-K^+ pump can form a net outward current that affects the pacemaker activity [61]; for instance, a previous study recorded Na^+-K^+ pump current-mediated membrane hyperpolarization in rabbit SA node cells [62]. More importantly, the Na^+-K^+ pump activity is increased by β-adrenoceptor-mediated phosphorylation of phospholamban, a small

sarcolemmal protein [63].

We confirmed and expanded upon these previous findings, demonstrating the contribution of the I_{Ks} channel to PVC automaticity under both control (basal) and β-adrenoceptors activation conditions. Blockade of I_{Ks} by its selective inhibitor is more effective after β-adrenoceptors stimulation than in control settings, indicating the critical modulation of I_{Ks} in the formation of automaticity when sympathetic tone is promoted. Our findings are supported by previous studies. For example, in guinea pig ventricular myocytes, the slow deactivation of I_{Ks} resulted in an increase in the relative contribution of the current at faster stimulation frequencies, as there is less time to allow for complete deactivation [64]. In addition, the contribution of I_{Ks} is less marked at normal heart rates, but under sympathetic stimulation, the current is upregulated by slowing the rate of deactivation [49]. The frequency-dependent potentiation of I_{Ks} is called "repolarization reserve" and can shorten the duration of action potential and ensure a sufficient time for ventricular filling [65, 66]. In addition, a recent report showed that I_{Kr} makes a prominent contribution to the cardiac action potentials, however, the I_{Kr}–I_{Ks} dominant pattern was reversed under β-adrenergic stimulation conditions [26]. In addition, it should be noted that I_f was reported in the PVC of rat and guinea pig [67]. Importantly, in SA node cells the I_f current regulates the heart rate under both

physiological and β-adrenoceptor-stimulated conditions [60, 61]. As shown in these reports, a rise in intracellular cAMP induced by a β-adrenoceptor agonist (e.g., isoproterenol) positively shifts the voltage-dependence of I_f activation, thereby providing more inward current during diastolic depolarization and accelerating pacemaker activity [60, 68].

There is increasing evidence showing that abnormal activity and modification of the sympathetic and parasympathetic functions are involved in the pathogenesis of AF [69]. An interesting recent study reported by Kato [70] showed that, in rabbit ventricular myocardium, the spiral-wave reentry is maintained by β-adrenergic stimulation, likely through enhancement of I_{Ks}. Because this effect was reversed by I_{Ks} inhibitor, the authors suggested that blockade of I_{Ks} channels might be a promising therapeutic modality under conditions of high sympathetic activity.

The present study showed that an elevated sympathetic tone is accompanied by an enhancement of voltage-dependent outward K^+ current through I_{Ks} in guinea pig PVC. Taken together with previous observations, these results form an important electrophysiological basis for insight into the regulatory mechanisms for ion channels in PVC under physiological basal conditions and during sympathetic stimulation. Thus, in PVC, upregulation of the I_{Ks}

channel by both α_1- and β_2-adrenoceptors (mainly) appears to be a potential pharmacological target for the treatment of AF originating from the PVs.

Sources of Funding

This study was supported by a Grant-in-Aid for Scientific Research (No. 17K08536 to H.M.) from the Japan Society for the Promotion of Science (Tokyo, Japan).

Author contributions

W-G. D., XY. M. and H. M. designed the experiments. XY. M., W-G. D. and M. O-K. conducted the experiments. XY. M., W-G. D., F. T. and A. K. participated in the data interpretation. XY. M., W-G. D. and H. M. wrote the manuscript. XY. M. W-G. D., F. T., A. K., M. O-K. and H. M. approved the final manuscript.

Conflict of interest

The authors declare no conflicts of interest.

Data availability

The data that support the findings of this study are available from the corresponding

author upon reasonable request.

References

[1] S. Nattel, D. Dobrev, Electrophysiological and molecular mechanisms of paroxysmal atrial fibrillation, Nature Reviews Cardiology 13(10) (2016) 575-590.

[2] D.W. Cheung, Electrical activity of the pulmonary vein and its interaction with the right atrium in the guinea-pig, The Journal of physiology 314 (1981) 445-56.

[3] D.W. Cheung, Pulmonary vein as an ectopic focus in digitalis-induced arrhythmia, Nature 294(5841) (1981) 582-4.

[4] M. Haïssaguerre, P. Jaïs, D.C. Shah, A. Takahashi, M. Hocini, G. Quiniou, S. Garrigue, A. Le Mouroux, P. Le Métayer, J. Clémenty, Spontaneous initiation of atrial fibrillation by ectopic beats originating in the pulmonary veins, The New England journal of medicine 339(10) (1998) 659-66.

[5] S. Nattel, Basic electrophysiology of the pulmonary veins and their role in atrial fibrillation: precipitators, perpetuators, and perplexers, Journal of cardiovascular electrophysiology 14(12) (2003) 1372-5.

[6] I. Namekata, Y. Tsuneoka, H. Tanaka, Electrophysiological and pharmacological properties of the pulmonary vein myocardium, Biological & pharmaceutical bulletin 36(1) (2013) 2-7.

[7] P. Jaïs, M. Haïssaguerre, D.C. Shah, S. Chouairi, L. Gencel, M. Hocini, J. Clémenty, A focal source of atrial fibrillation treated by discrete radiofrequency ablation, Circulation 95(3) (1997) 572-6.

[8] H. Calkins, Has the time come to abandon the concept that "pulmonary vein isolation is the cornerstone of atrial fibrillation ablation"?, Circulation. Arrhythmia and electrophysiology 6(2) (2013) 241-2.

[9] P. Melnyk, J.R. Ehrlich, M. Pourrier, L. Villeneuve, T.J. Cha, S. Nattel, Comparison of ion channel distribution and expression in cardiomyocytes of canine pulmonary veins versus left atrium, Cardiovascular research 65(1) (2005) 104-16.

[10] L.W. Lo, Y.C. Chen, Y.J. Chen, W. Wongcharoen, C.I. Lin, S.A. Chen, Calmodulin kinase II inhibition prevents arrhythmic activity induced by alpha and beta adrenergic agonists in rabbit pulmonary veins, European journal of pharmacology 571(2-3) (2007) 197-208.

[11] Y. Okamoto, M. Takano, T. Ohba, K. Ono, Arrhythmogenic coupling between the Na+ -Ca2+ exchanger and inositol 1,4,5-triphosphate receptor in rat pulmonary vein cardiomyocytes, Journal of molecular and cellular cardiology 52(5) (2012) 988-97.

[12] V. Maupoil, C. Bronquard, J.L. Freslon, P. Cosnay, I. Findlay, Ectopic activity in the rat pulmonary vein can arise from simultaneous activation of alpha1- and beta1-adrenoceptors, British journal of pharmacology 150(7) (2007) 899-905.

[13] Y. Tsuneoka, M. Irie, Y. Tanaka, T. Sugimoto, Y. Kobayashi, T. Kusakabe, K. Kato, S. Hamaguchi, I. Namekata, H. Tanaka, Permissive role of reduced inwardly-rectifying potassium current density in the automaticity of the guinea pig pulmonary vein myocardium, Journal of pharmacological sciences 133(4) (2017) 195-202.

[14] M. Irie, Y. Tsuneoka, M. Shimobayashi, N. Hasegawa, Y. Tanaka, S. Mochizuki, S. Ichige, S. Hamaguchi, I. Namekata, H. Tanaka, Involvement of alpha- and beta-adrenoceptors in the automaticity of the isolated guinea pig pulmonary vein myocardium, Journal of pharmacological sciences 133(4) (2017) 247-253.

[15] M. Hocini, S.Y. Ho, T. Kawara, A.C. Linnenbank, M. Potse, D. Shah, P. Jaïs, M.J. Janse, M. Haïssaguerre, J.M. De Bakker, Electrical conduction in canine pulmonary veins:

electrophysiological and anatomic correlation, Circulation 105(20) (2002) 2442-8.

[16] J.R. Ehrlich, T.J. Cha, L. Zhang, D. Chartier, P. Melnyk, S.H. Hohnloser, S. Nattel, Cellular electrophysiology of canine pulmonary vein cardiomyocytes: action potential and ionic current properties, The Journal of physiology 551(Pt 3) (2003) 801-13.

[17] I. Namekata, Y. Tsuneoka, A. Takahara, H. Shimada, T. Sugimoto, K. Takeda, M. Nagaharu, K. Shigenobu, T. Kawanishi, H. Tanaka, Involvement of the Na(+)/Ca(2+) exchanger in the automaticity of guinea-pig pulmonary vein myocardium as revealed by SEA0400, Journal of pharmacological sciences 110(1) (2009) 111-6.

[18] M.C. Sanguinetti, N.K. Jurkiewicz, Two components of cardiac delayed rectifier K+ current. Differential sensitivity to block by class III antiarrhythmic agents, The Journal of general physiology 96(1) (1990) 195-215.

[19] M.C. Sanguinetti, M.E. Curran, A. Zou, J. Shen, P.S. Spector, D.L. Atkinson, M.T. Keating, Coassembly of K(V)LQT1 and minK (IsK) proteins to form cardiac I(Ks) potassium channel, Nature 384(6604) (1996) 80-3.

[20] J. Barhanin, F. Lesage, E. Guillemare, M. Fink, M. Lazdunski, G. Romey, K(V)LQT1 and lsK (minK) proteins associate to form the I(Ks) cardiac potassium current, Nature 384(6604) (1996) 78-80.

[21] R.F. Bosch, A.C. Schneck, S. Csillag, B. Eigenberger, U. Gerlach, J. Brendel, H.J. Lang, C. Mewis, H. Gögelein, L. Seipel, V. Kühlkamp, Effects of the chromanol HMR 1556 on potassium currents in atrial myocytes, Naunyn-Schmiedeberg's archives of pharmacology 367(3) (2003) 281-8.

[22] R.F. Bosch, R. Gaspo, A.E. Busch, H.J. Lang, G.R. Li, S. Nattel, Effects of the chromanol 293B, a selective blocker of the slow, component of the delayed rectifier K+

current, on repolarization in human and guinea pig ventricular myocytes, Cardiovascular research 38(2) (1998) 441-50.

[23] H. Irisawa, H.F. Brown, W. Giles, Cardiac pacemaking in the sinoatrial node, Physiological reviews 73(1) (1993) 197-227.

[24] Y. Xie, W.G. Ding, H. Matsuura, Ca2+/calmodulin potentiates I Ks in sinoatrial node cells by activating Ca2+/calmodulin-dependent protein kinase II, Pflugers Archiv : European journal of physiology 467(2) (2015) 241-51.

[25] H. Matsuura, T. Ehara, W.G. Ding, M. Omatsu-Kanbe, T. Isono, Rapidly and slowly activating components of delayed rectifier K(+) current in guinea-pig sino-atrial node pacemaker cells, The Journal of physiology 540(Pt 3) (2002) 815-30.

[26] T. Banyasz, Z. Jian, B. Horvath, S. Khabbaz, L.T. Izu, Y. Chen-Izu, Beta-adrenergic stimulation reverses the I Kr-I Ks dominant pattern during cardiac action potential, Pflugers Archiv : European journal of physiology 466(11) (2014) 2067-76.

[27] M. Si, J. Xu, F. Zhang, C. Wang, X. Du, H. Zhang, Involvement of protein kinase A and C in norepinephrine- and angiotensin II-induced modulation of cardiac IKs, Pharmacology 92(3-4) (2013) 217-26.

[28] M.C. Sanguinetti, N.K. Jurkiewicz, Delayed rectifier outward K+ current is composed of two currents in guinea pig atrial cells, The American journal of physiology 260(2 Pt 2) (1991) H393-9.

[29] W.G. Ding, F. Toyoda, H. Matsuura, Blocking action of chromanol 293B on the slow component of delayed rectifier K(+) current in guinea-pig sino-atrial node cells, British journal of pharmacology 137(2) (2002) 253-62.

[30] Z. Wang, B. Fermini, S. Nattel, Rapid and slow components of delayed rectifier current

in human atrial myocytes, Cardiovascular research 28(10) (1994) 1540-6.

[31] R.P. Xiao, W. Zhu, M. Zheng, C. Cao, Y. Zhang, E.G. Lakatta, Q. Han, Subtype-specific alpha1- and beta-adrenoceptor signaling in the heart, Trends in pharmacological sciences 27(6) (2006) 330-7.

[32] Y. Xiang, B.K. Kobilka, Myocyte adrenoceptor signaling pathways, Science (New York, N.Y.) 300(5625) (2003) 1530-2.

[33] N. Percie du Sert, A. Ahluwalia, S. Alam, M.T. Avey, M. Baker, W.J. Browne, A. Clark, I.C. Cuthill, U. Dirnagl, M. Emerson, P. Garner, S.T. Holgate, D.W. Howells, V. Hurst, N.A. Karp, S.E. Lazic, K. Lidster, C.J. MacCallum, M. Macleod, E.J. Pearl, O.H. Petersen, F. Rawle, P. Reynolds, K. Rooney, E.S. Sena, S.D. Silberberg, T. Steckler, H. Würbel, Reporting animal research: Explanation and elaboration for the ARRIVE guidelines 2.0, PLoS biology 18(7) (2020) e3000411.

[34] A. Marcantoni, V. Carabelli, D.H. Vandael, V. Comunanza, E. Carbone, PDE type-4 inhibition increases L-type Ca(2+) currents, action potential firing, and quantal size of exocytosis in mouse chromaffin cells, Pflugers Archiv : European journal of physiology 457(5) (2009) 1093-110.

[35] A.J. Kaumann, H. Lemoine, Beta 2-adrenoceptor-mediated positive inotropic effect of adrenaline in human ventricular myocardium. Quantitative discrepancies with binding and adenylate cyclase stimulation, Naunyn-Schmiedeberg's archives of pharmacology 335(4) (1987) 403-11.

[36] L.P. Collis, S. Srivastava, W.A. Coetzee, M. Artman, beta2-Adrenergic receptor agonists stimulate L-type calcium current independent of PKA in newborn rabbit ventricular myocytes, American journal of physiology. Heart and circulatory physiology 293(5) (2007) H2826-35.

[37] J.P. Bénitah, A.M. Gomez, P. Bailly, J.P. Da Ponte, G. Berson, C. Delgado, P. Lorente, Heterogeneity of the early outward current in ventricular cells isolated from normal and hypertrophied rat hearts, The Journal of physiology 469 (1993) 111-38.

[38] W.G. Ding, Y. Xie, F. Toyoda, H. Matsuura, Improved functional expression of human cardiac kv1.5 channels and trafficking-defective mutants by low temperature treatment, PloS one 9(3) (2014) e92923.

[39] Y. Li, T. Hof, T.A. Baldwin, L. Chen, R.S. Kass, C.W. Dessauer, Regulation of I(Ks) Potassium Current by Isoproterenol in Adult Cardiomyocytes Requires Type 9 Adenylyl Cyclase, Cells 8(9) (2019).

[40] I. Piccini, E. Fehrmann, S. Frank, F.U. Müller, B. Greber, G. Seebohm, Adrenergic Stress Protection of Human iPS Cell-Derived Cardiomyocytes by Fast K(v)7.1 Recycling, Frontiers in physiology 8 (2017) 705.

[41] Z.A. McCrossan, T.K. Roepke, A. Lewis, G. Panaghie, G.W. Abbott, Regulation of the Kv2.1 potassium channel by MinK and MiRP1, The Journal of membrane biology 228(1) (2009) 1-14.

[42] R.P. Xiao, P. Avdonin, Y.Y. Zhou, H. Cheng, S.A. Akhter, T. Eschenhagen, R.J. Lefkowitz, W.J. Koch, E.G. Lakatta, Coupling of beta2-adrenoceptor to Gi proteins and its physiological relevance in murine cardiac myocytes, Circulation research 84(1) (1999) 43-52.

[43] R.P. Xiao, X. Ji, E.G. Lakatta, Functional coupling of the beta 2-adrenoceptor to a pertussis toxin-sensitive G protein in cardiac myocytes, Molecular pharmacology 47(2) (1995) 322-9.

[44] P. Molenaar, S. Bartel, A. Cochrane, D. Vetter, H. Jalali, P. Pohlner, K. Burrell, P. Karczewski, E.G. Krause, A. Kaumann, Both beta(2)- and beta(1)-adrenergic receptors

mediate hastened relaxation and phosphorylation of phospholamban and troponin I in ventricular myocardium of Fallot infants, consistent with selective coupling of beta(2)-adrenergic receptors to G(s)-protein, Circulation 102(15) (2000) 1814-21.

[45] A. Kaumann, S. Bartel, P. Molenaar, L. Sanders, K. Burrell, D. Vetter, P. Hempel, P. Karczewski, E.G. Krause, Activation of beta2-adrenergic receptors hastens relaxation and mediates phosphorylation of phospholamban, troponin I, and C-protein in ventricular myocardium from patients with terminal heart failure, Circulation 99(1) (1999) 65-72.

[46] A.J. Kaumann, L. Sanders, J.A. Lynham, S. Bartel, M. Kuschel, P. Karczewski, E.G. Krause, Beta 2-adrenoceptor activation by zinterol causes protein phosphorylation, contractile effects and relaxant effects through a cAMP pathway in human atrium, Molecular and cellular biochemistry 163-164 (1996) 113-23.

[47] M. Kuschel, Y.Y. Zhou, H.A. Spurgeon, S. Bartel, P. Karczewski, S.J. Zhang, E.G. Krause, E.G. Lakatta, R.P. Xiao, beta2-adrenergic cAMP signaling is uncoupled from phosphorylation of cytoplasmic proteins in canine heart, Circulation 99(18) (1999) 2458-65.

[48] V.A. Kanda, K. Purtell, G.W. Abbott, Protein kinase C downregulates I(Ks) by stimulating KCNQ1-KCNE1 potassium channel endocytosis, Heart rhythm 8(10) (2011) 1641-7.

[49] C. Terrenoire, C.E. Clancy, J.W. Cormier, K.J. Sampson, R.S. Kass, Autonomic control of cardiac action potentials: role of potassium channel kinetics in response to sympathetic stimulation, Circulation research 96(5) (2005) e25-34.

[50] K.W. Dilly, J. Kurokawa, C. Terrenoire, S. Reiken, W.J. Lederer, A.R. Marks, R.S. Kass, Overexpression of beta2-adrenergic receptors cAMP-dependent protein kinase phosphorylates and modulates slow delayed rectifier potassium channels expressed in murine

heart: evidence for receptor/channel co-localization, The Journal of biological chemistry 279(39) (2004) 40778-87.

[51] E. Thompson, J. Eldstrom, M. Westhoff, D. McAfee, E. Balse, D. Fedida, cAMP-dependent regulation of I(Ks) single-channel kinetics, The Journal of general physiology 149(8) (2017) 781-798.

[52] Y. Xiang, V.O. Rybin, S.F. Steinberg, B. Kobilka, Caveolar localization dictates physiologic signaling of beta 2-adrenoceptors in neonatal cardiac myocytes, The Journal of biological chemistry 277(37) (2002) 34280-6.

[53] V.O. Rybin, X. Xu, M.P. Lisanti, S.F. Steinberg, Differential targeting of beta -adrenergic receptor subtypes and adenylyl cyclase to cardiomyocyte caveolae. A mechanism to functionally regulate the cAMP signaling pathway, The Journal of biological chemistry 275(52) (2000) 41447-57.

[54] M.R. Bristow, R. Ginsburg, V. Umans, M. Fowler, W. Minobe, R. Rasmussen, P. Zera, R. Menlove, P. Shah, S. Jamieson, et al., Beta 1- and beta 2-adrenergic-receptor subpopulations in nonfailing and failing human ventricular myocardium: coupling of both receptor subtypes to muscle contraction and selective beta 1-receptor down-regulation in heart failure, Circulation research 59(3) (1986) 297-309.

[55] J.A. Hall, A.J. Kaumann, M.J. Brown, Selective beta 1-adrenoceptor blockade enhances positive inotropic responses to endogenous catecholamines mediated through beta 2-adrenoceptors in human atrial myocardium, Circulation research 66(6) (1990) 1610-23.

[56] E. Gille, H. Lemoine, B. Ehle, A.J. Kaumann, The affinity of (-)-propranolol for beta 1- and beta 2-adrenoceptors of human heart. Differential antagonism of the positive inotropic effects and adenylate cyclase stimulation by (-)-noradrenaline and (-)-adrenaline,

Naunyn-Schmiedeberg's archives of pharmacology 331(1) (1985) 60-70.

[57] G. Engel, Subclasses of beta-adrenoceptors--a quantitative estimation of beta 1- and beta 2- adrenoceptors in guinea pig and human lung, Postgraduate medical journal 57 Suppl 1 (1981) 77-83.

[58] Y.J. Chen, S.A. Chen, Y.C. Chen, H.I. Yeh, M.S. Chang, C.I. Lin, Electrophysiology of single cardiomyocytes isolated from rabbit pulmonary veins: implication in initiation of focal atrial fibrillation, Basic research in cardiology 97(1) (2002) 26-34.

[59] Y.J. Chen, S.A. Chen, Y.C. Chen, H.I. Yeh, P. Chan, M.S. Chang, C.I. Lin, Effects of rapid atrial pacing on the arrhythmogenic activity of single cardiomyocytes from pulmonary veins: implication in initiation of atrial fibrillation, Circulation 104(23) (2001) 2849-54.

[60] D. DiFrancesco, Pacemaker mechanisms in cardiac tissue, Annual review of physiology 55 (1993) 455-72.

[61] M.E. Mangoni, J. Nargeot, Genesis and regulation of the heart automaticity, Physiological reviews 88(3) (2008) 919-82.

[62] A. Noma, H. Irisawa, Contribution of an electrogenic sodium pump to the membrane potential in rabbit sinoatrial node cells, Pflugers Archiv : European journal of physiology 358(4) (1975) 289-301.

[63] D.M. Bers, S. Despa, Na/K-ATPase--an integral player in the adrenergic fight-or-flight response, Trends in cardiovascular medicine 19(4) (2009) 111-8.

[64] B.M. Heath, D.A. Terrar, The deactivation kinetics of the delayed rectifier components IKr and IKs in guinea-pig isolated ventricular myocytes, Experimental physiology 81(4) (1996) 605-21.

[65] M. Stengl, P.G. Volders, M.B. Thomsen, R.L. Spätjens, K.R. Sipido, M.A. Vos,

Accumulation of slowly activating delayed rectifier potassium current (IKs) in canine ventricular myocytes, The Journal of physiology 551(Pt 3) (2003) 777-86.

[66] J. Silva, Y. Rudy, Subunit interaction determines IKs participation in cardiac repolarization and repolarization reserve, Circulation 112(10) (2005) 1384-91.

[67] D. Takagi, Y. Okamoto, T. Ohba, H. Yamamoto, K. Ono, Comparative study of hyperpolarization-activated currents in pulmonary vein cardiomyocytes isolated from rat, guinea pig, and rabbit, The journal of physiological sciences : JPS 70(1) (2020) 6.

[68] M.E. Mangoni, B. Couette, L. Marger, E. Bourinet, J. Striessnig, J. Nargeot, Voltage-dependent calcium channels and cardiac pacemaker activity: from ionic currents to genes, Progress in biophysics and molecular biology 90(1-3) (2006) 38-63.

[69] A.A. Khan, G.Y.H. Lip, A. Shantsila, Heart rate variability in atrial fibrillation: The balance between sympathetic and parasympathetic nervous system, European journal of clinical investigation 49(11) (2019) e13174.

[70] S. Kato, H. Honjo, Y. Takemoto, H. Takanari, T. Suzuki, Y. Okuno, T. Opthof, I. Sakuma, S. Inada, K. Nakazawa, T. Ashihara, I. Kodama, K. Kamiya, Pharmacological blockade of IKs destabilizes spiral-wave reentry under β-adrenergic stimulation in favor of its early termination, Journal of pharmacological sciences 119(1) (2012) 52-63.

Figure legends

Figure 1. Expression, localization and current density of I_{Ks} in PVC and LA. (A) Western blot image showing I_{Ks} (*KCNQ1*) protein, detected as a single band at approximately 100 kDa in size. (B) The differing current densities of I_{Ks} in PVC (n = 16, N = 8) and LA (n = 6, N = 6). (C) Immunocytochemical staining of I_{Ks} in PVC (upper panel) and LA (lower panel) in three-dimensional images, membrane maker images and merged with *KCNQ1* images. DAPI was used for nuclear staining. DIC, differential interference contrast. Note that the same *KCNQ1* antibody was used for immunocytochemistry and Western blotting. Data represent the mean ± S.E.M., the number of technical replicates is indicated in the respective bars. Student's t-test was used to compare the density of the tail current; *, P <0.05.

Figure 2. The effects of isoproterenol and norepinephrine on I_{Ks} current activity. (A) Superimposed traces of I_{Ks} during steps to test potentials of -50 to +40 mV applied from a holding potential of -50 mV before and 5 min after the application of isoproterenol (non-selective β-agonist, 0.1 μM). (B) Mean *I-V* relationships for the I_{Ks} current in the absence and presence of isoproterenol (n = 6, N = 6; n = 6, N = 6). (C) Voltage dependence of I_{Ks} activation for normalized tail currents in the absence and presence of isoproterenol (n = 6,

N = 6; n = 6, N = 6). The smooth curves through the data points were fitted to a Boltzmann equation, yielding $V_{1/2}$ and k for I_{Ks}. (D) Superimposed traces of I_{Ks} obtained by the same protocol as shown in A, before and 5 min after the application of norepinephrine (adrenoceptor agonist, 5 μM). (E) Mean *I-V* relationships for the I_{Ks} current in the absence and presence of norepinephrine (n = 6, N = 5; n = 6, N = 5). (F) Voltage dependence of I_{Ks} activation for normalized tail currents in the absence and presence of norepinephrine (n = 6, N = 5; n = 6, N = 5). The smooth curves through the data points were fitted to a Boltzmann equation, yielding $V_{1/2}$ and k for I_{Ks}. (G) Mean data for the rate of increase in the I_{Ks} current induced by isoproterenol (n = 13, N = 7) and norepinephrine (n = 13, N = 6). (H) Changes in the $V_{1/2}$ induced by treatment with isoproterenol (n = 6, N = 6) and norepinephrine (n = 6, N = 5). Data represent the mean ± S.E.M., the number of technical replicates indicated is indicated in respective bars. One-way ANOVA (Tukey correction) was used to compare the increase rate of tail current and change of $V_{1/2}$ in G and H; *, P <0.05.

Figure 3. The effect of β$_1$-agonist stimulation on I_{Ks} current activity. (A) I_{Ks} current obtained before and 5 min after the application of denopamine (β$_1$-agonist, 1 μM) in the presence of ICI 118551 (selective β$_2$-adrenoceptor inhibitor, 0.1 μM). (B) Mean *I-V*

relationships for the I_{Ks} tail current in the absence and presence of denopamine (n = 6, N = 6; n = 6, N = 6). (C) Voltage dependence of I_{Ks} activation for normalized tail currents in the absence and presence of isoproterenol (n = 6, N = 6; n = 6, N = 6), fitted to a Boltzmann equation. Data represent the mean ± S.E.M., the number of technical replicates indicated is indicated in respective bars.

Figure 4. The comparison of I_{Ks} enhancement under β_1- and β_2-adrenoceptor stimulation. (A) I_{Ks} current recorded before and 5 min after the application of zinterol (β_2-agonist, 1 μM) in the presence of CGP 20712A (selective β_1-adrenoceptor inhibitor, 0.3 μM). (B and C) Mean *I-V* relationships for the I_{Ks} tail current and the voltage dependence of I_{Ks} activation in the absence and presence of zinterol throughout with CGP 20712A (n = 6, N = 6; n = 6, N = 6). (D) I_{Ks} current recorded before and 5 min after the application of zinterol in the presence of ICI 118551. (E and F) Mean *I-V* relationships for the I_{Ks} tail current and the voltage dependence of I_{Ks} activation in the absence and presence of zinterol throughout with ICI 118551 (n = 6, N = 5; n = 6, N = 5). (G) The rates of increase in I_{Ks} induced by denopamine (n = 10, N = 8) and zinterol (n = 9, N = 7) in the presence of β_2- or β_1-adrenoceptor inhibitor, respectively. (H) Changes in $V_{1/2}$ obtained from different

treatments with β_1- or β_2-adrenoceptor agonists (n = 6, N = 6; n = 6, N = 6). Data represent the mean ± S.E.M., the number of technical replicates is indicated in the respective bars. Student's t-test was used to compare the increase rate of tail current and change of $V_{1/2}$ in G and H; *, P <0.05.

Figure 5. Involvement of the AC-cAMP-PKA signaling pathway in β_1- and β_2-adrenoceptor-mediated I_{Ks} potentiation. (A) I_{Ks} current recorded before and 5 min after the application of denopamine (1 μM) in the continuous presence of ICI 118551 (0.1 μM) plus H89 (selective PKA inhibitor, 25 μM). (B) I_{Ks} current recorded before and 5 min after the application of zinterol (1 μM) in the continuous presence of CGP 20712A (0.3 μM) plus H89. (C) I_{Ks} current recorded before and 5 min after the application of denopamine in the continuous presence of ICI 118551 plus SQ 22536 (AC inhibitor, 300 μM). (D) I_{Ks} current recorded before and 5 min after the application of zinterol in the continuous presence of CGP 20712A plus SQ 22536. (E and F) Summarized data for the rates of increase in I_{Ks} induced by denopamine and zinterol under pre-treatment with H89 (n = 9, N = 7; n = 9, N = 7) or SQ 22536 (n = 8, N = 6; n = 8, N = 7), respectively. Note that the data related to the application of denopamine and zinterol (panels E and F) were obtained from the same data shown in

Figure 4G. Data represent the mean ± S.E.M., the number of technical replicates indicated is indicated in respective bars. One-way ANOVA (Tukey correction) was used to compare the increase rate of tail current in E and F; *, P <0.05.

Figure 6. Involvement of the PKC pathway in the α_1-adrenoceptor-induced increase in I_{Ks}. (A) I_{Ks} current obtained before and 5 min after the application of phenylephrine (selective α_1-agonist, 30 μM). (B and C) Mean *I-V* relationships for the I_{Ks} tail current and the voltage dependence of I_{Ks} activation in the absence and presence of α_1-adrenoceptor stimulation (n = 6, N = 6; n = 6, N = 6), respectively. (D) I_{Ks} current recorded before and 5 min after the application of phenylephrine in the continuous presence of BIS-I (selective PKC inhibitor, 0.5 μM). (E) Summarized data for the rates of increase in I_{Ks} following phenylephrine treatment in the absence and presence of BIS-I (n = 12, N = 8; n = 12, N = 8), respectively. Data represent the mean ± S.E.M., the number of technical replicates is indicated in the respective bars. Student's t-test was used to compare the density of the tail current in E; *, P <0.05.

Figure 7. Contribution of individual adrenoceptors activation to PVC automaticity. (A)

Action potentials on an expanded timescale recorded under control conditions and following the application of norepinephrine (5 μM) (B) Action potentials recorded in the absence and presence of norepinephrine with prazosin (2 μM) and ICI 118551 (0.1 μM). (C) Action potentials recorded in the absence and presence of norepinephrine with prazosin and CGP 20712A (0.3 μM). (D) Action potentials recorded in the absence and presence of norepinephrine with ICI 118551 and CGP 20712A. (E) Action potentials recorded in the absence and presence of zinterol (1 μM) with prazosin and CGP 20712A. (F) Summarized data showing the increase in firing rates induced by norepinephrine in the absence and presence of β_1-, β_2- and α_1-adrenoceptor inhibitors (n= 5, N = 4; n= 6, N = 4; n= 6, N = 4; n= 6, N = 5), respectively. (G) Summarized data showing the increase in the firing rates reduced by denopamine (n= 6, N = 4) and zinterol (n = 5, N = 4), respectively. Data represent the mean ± S.E.M., the number of technical replicates indicated is indicated in respective bars. One-way ANOVA (Tukey correction) was used to compare the contribution of individual adrenoceptors activation following the application of norepinephrine in F and Student's t-test was used to compare the contribution of β_1- and β_2-adrenoceptors activation in G; *, P <0.05.

Figure 8. Contribution of I_{Ks} to the PVC automaticity under basal and β-adrenergic

receptor-activated conditions. (A) Continuous recording of action potentials during exposure to selective I_{Ks} blocker HMR-1556 (1 μM) with a washout period (upper panel). Action potentials (lower panel) on an expanded timescale recorded under control (a), during the administration of HMR-1556 (b) and under washout conditions (c). (B) Continuous recording of action potentials during exposure to isoproterenol (0.1 μM) and with the additive application of HMR-1556 in the continuous presence of isoproterenol (upper panel). Action potentials (lower panel) on an expanded timescale recorded under control (a) conditions and during exposure to isoproterenol (b) and isoproterenol plus HMR-1556 (c). (C) Summarized data for the reduction in the firing rates induced by HMR-1556 in the absence (control; n = 6, N = 6) and presence of isoproterenol (n = 6, N = 6). Data represent the mean ± S.E.M., the number of technical replicates indicated is indicated in respective bars. One-way ANOVA (Tukey correction) was used to compare the increase of firing rate and Student's t-test was used to compare the reduction of firing rate by HMR-1556 in C; *, P <0.05.

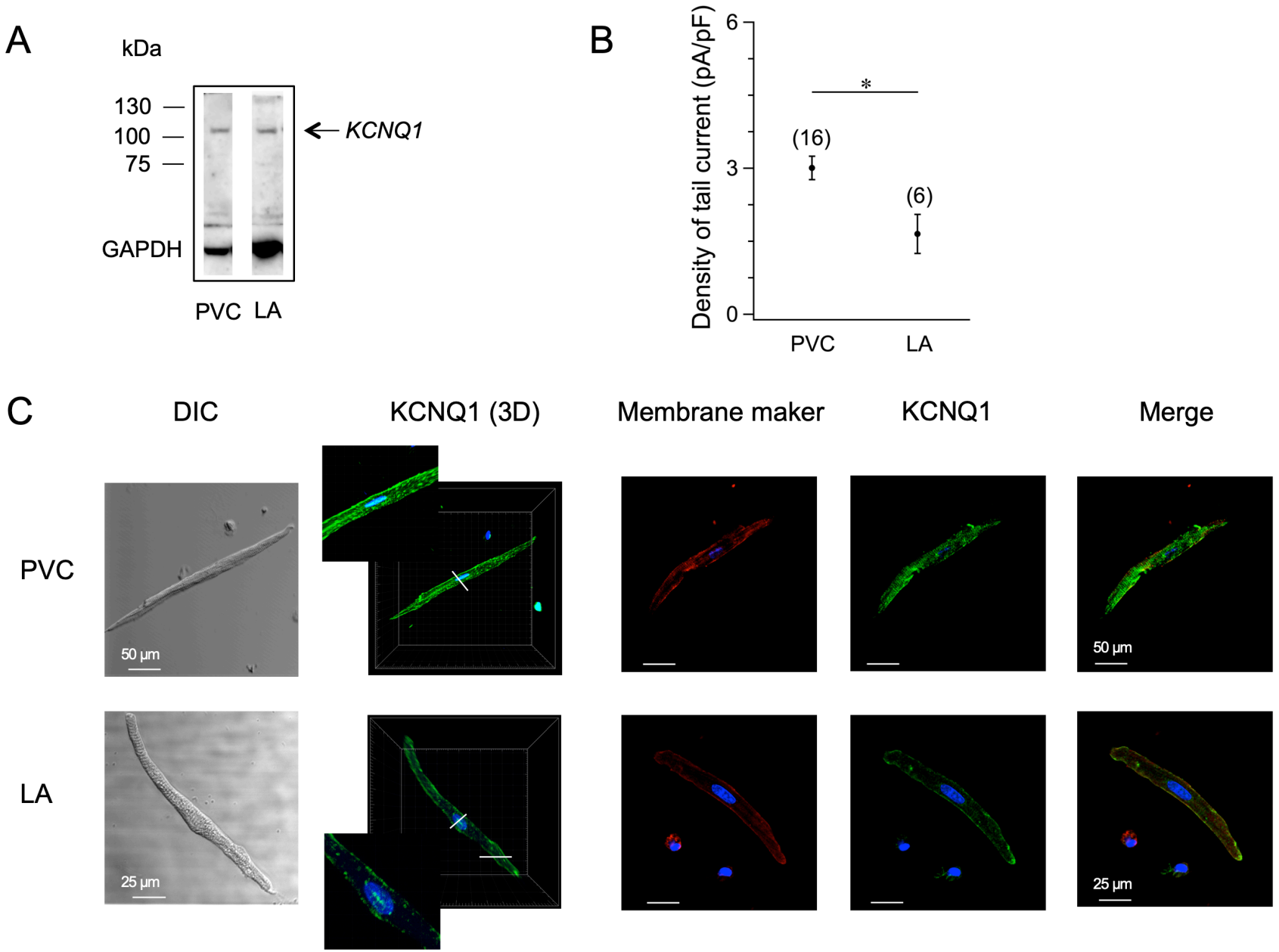
A
kDa
130
100
75
GAPDH
KCNQ1
PVC
LA
B
Density of tail current (pA/pF)
6
3
0
*
(16)
(6)
PVC
LA
C
DIC
KCNQ1 (3D)
Membrane maker
KCNQ1
Merge
PVC
LA
50 μm
25 μm
50 μm
25 μm

Fig. 1

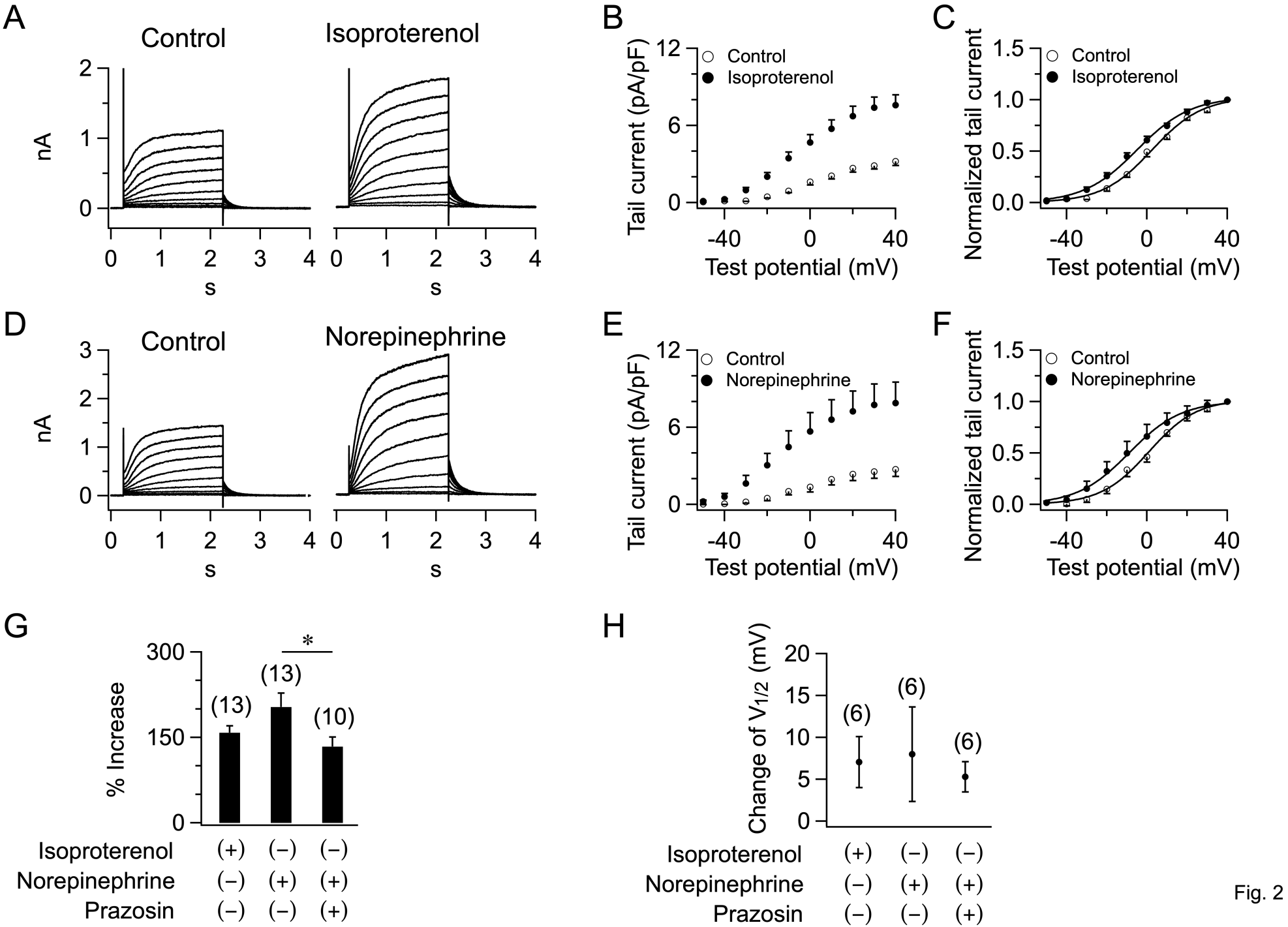
A
Control
Isoproterenol
nA
s
B
Control
Isoproterenol
Tail current (pA/pF)
Test potential (mV)
C
Control
Isoproterenol
Normalized tail current
Test potential (mV)
D
Control
Norepinephrine
nA
s
E
Control
Norepinephrine
Tail current (pA/pF)
Test potential (mV)
F
Control
Norepinephrine
Normalized tail current
Test potential (mV)
G
% Increase
(13)
(13)
(10)
*
Isoproterenol (+) (−) (−)
Norepinephrine (−) (+) (+)
Prazosin (−) (−) (+)
H
Change of $V_{1/2}$ (mV)
(6)
(6)
(6)
Isoproterenol (+) (−) (−)
Norepinephrine (−) (+) (+)
Prazosin (−) (−) (+)

Fig. 2

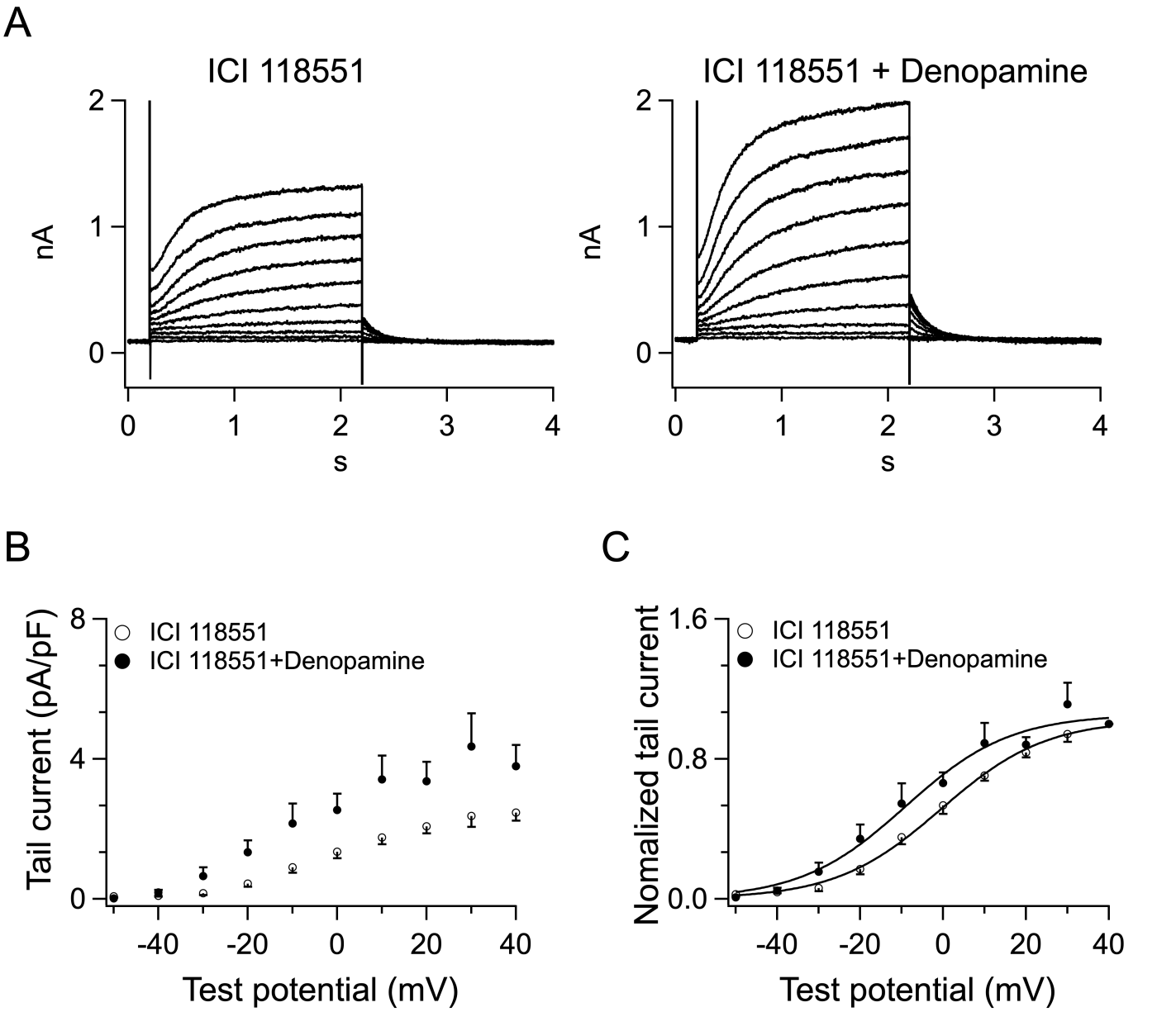
A
ICI 118551
ICI 118551 + Denopamine
nA
s
B
C
ICI 118551
ICI 118551+Denopamine
Tail current (pA/pF)
Test potential (mV)
Nomalized tail current

Fig. 3

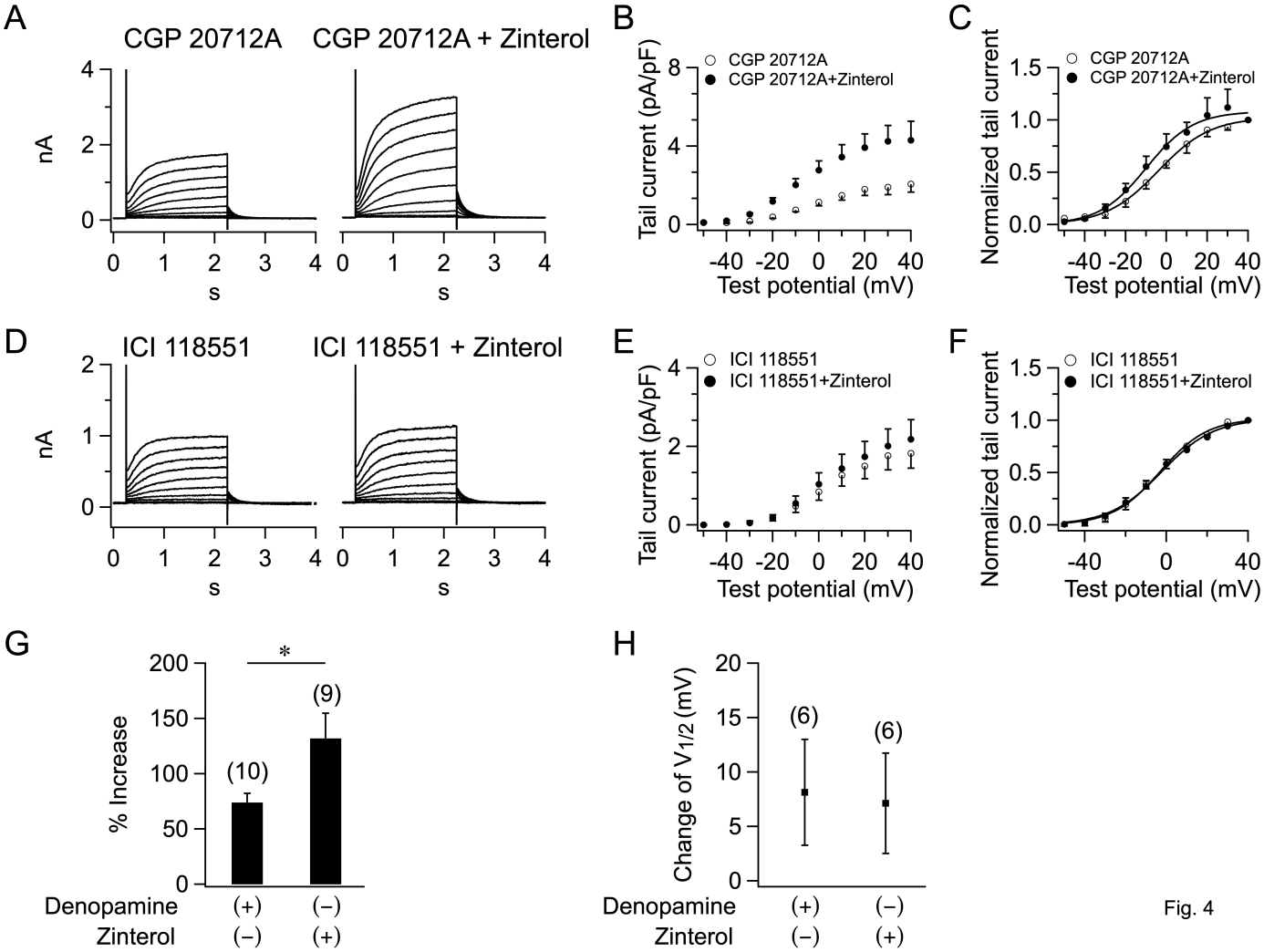
A
CGP 20712A
CGP 20712A + Zinterol
nA
s
B
CGP 20712A
CGP 20712A+Zinterol
Tail current (pA/pF)
Test potential (mV)
C
CGP 20712A
CGP 20712A+Zinterol
Normalized tail current
Test potential (mV)
D
ICI 118551
ICI 118551 + Zinterol
nA
s
E
ICI 118551
ICI 118551+Zinterol
Tail current (pA/pF)
Test potential (mV)
F
ICI 118551
ICI 118551+Zinterol
Normalized tail current
Test potential (mV)
G
% Increase
(10)
(9)
*
Denopamine (+) (−)
Zinterol (−) (+)
H
Change of V1/2 (mV)
(6)
(6)
Denopamine (+) (−)
Zinterol (−) (+)

Fig. 4

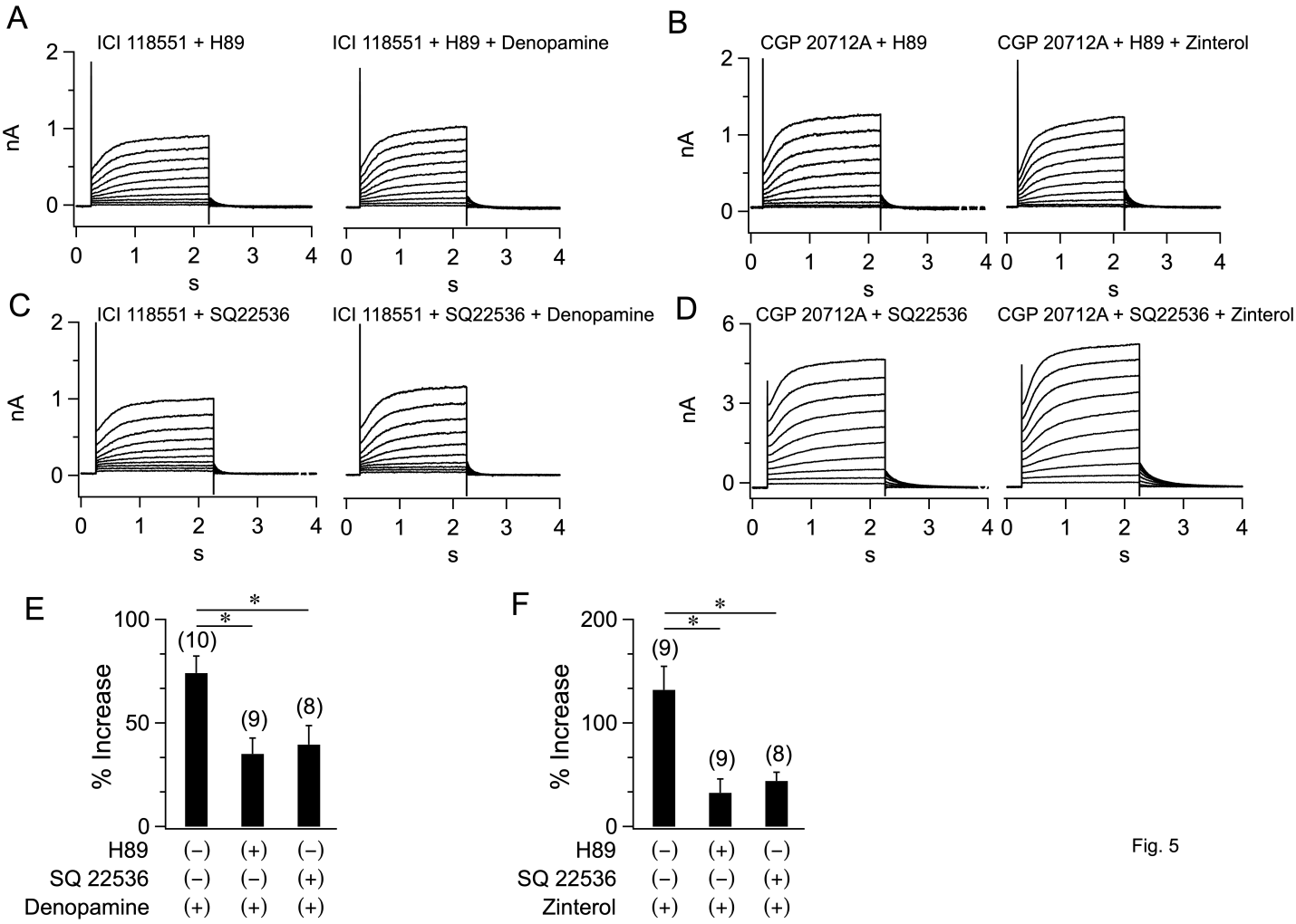
A
ICI 118551 + H89
ICI 118551 + H89 + Denopamine
nA
s
B
CGP 20712A + H89
CGP 20712A + H89 + Zinterol
C
ICI 118551 + SQ22536
ICI 118551 + SQ22536 + Denopamine
D
CGP 20712A + SQ22536
CGP 20712A + SQ22536 + Zinterol
E
% Increase
(10)
(9)
(8)
H89 (–) (+) (–)
SQ 22536 (–) (–) (+)
Denopamine (+) (+) (+)
F
Zinterol (+) (+) (+)

Fig. 5

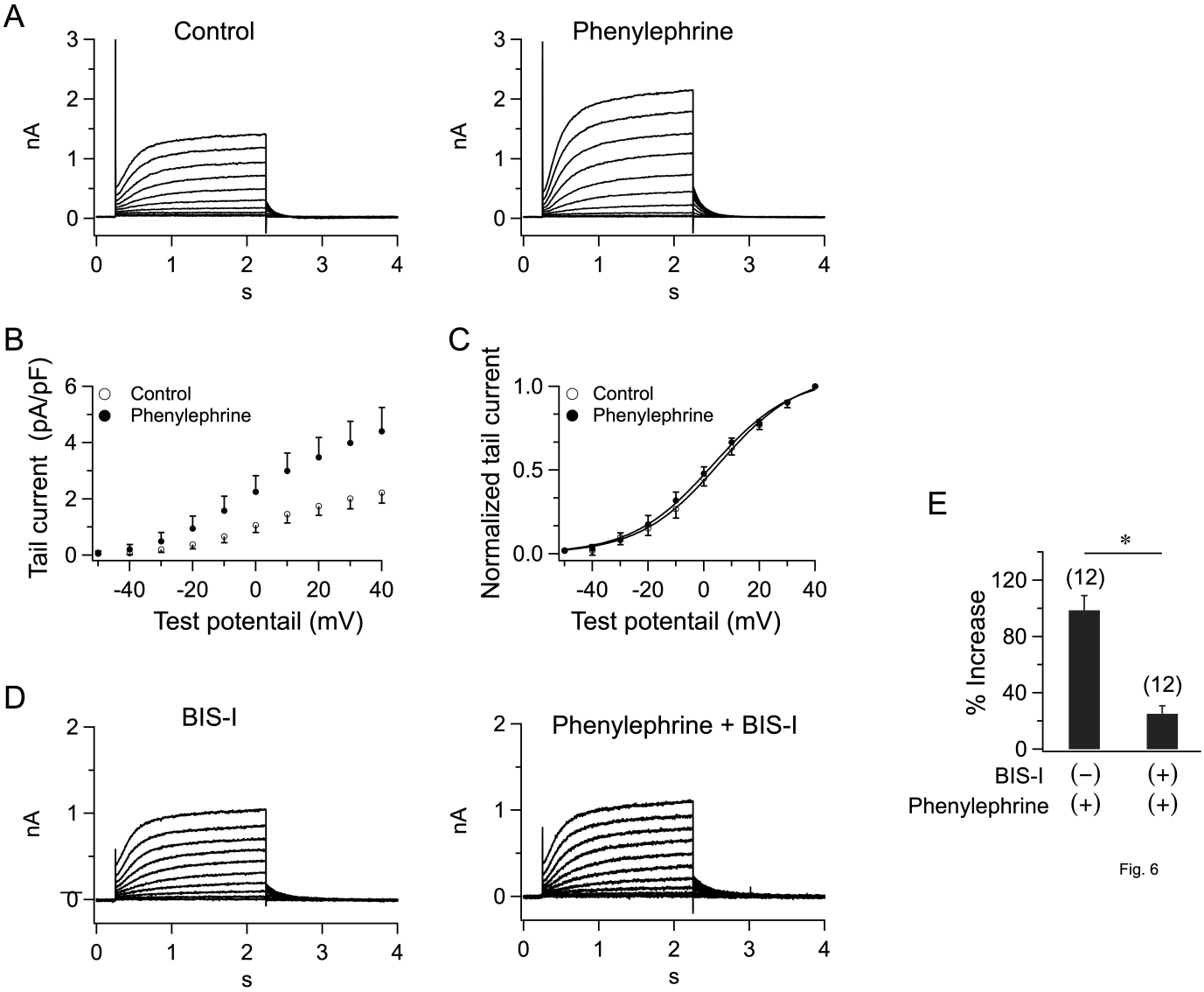
A
Control
Phenylephrine
nA
s
B
Control
Phenylephrine
Tail current (pA/pF)
Test potentail (mV)
C
Control
Phenylephrine
Normalized tail current
Test potentail (mV)
D
BIS-I
Phenylephrine + BIS-I
nA
s

E
*
(12)
(12)
% Increase
BIS-I (−) (+)
Phenylephrine (+) (+)

Fig. 6

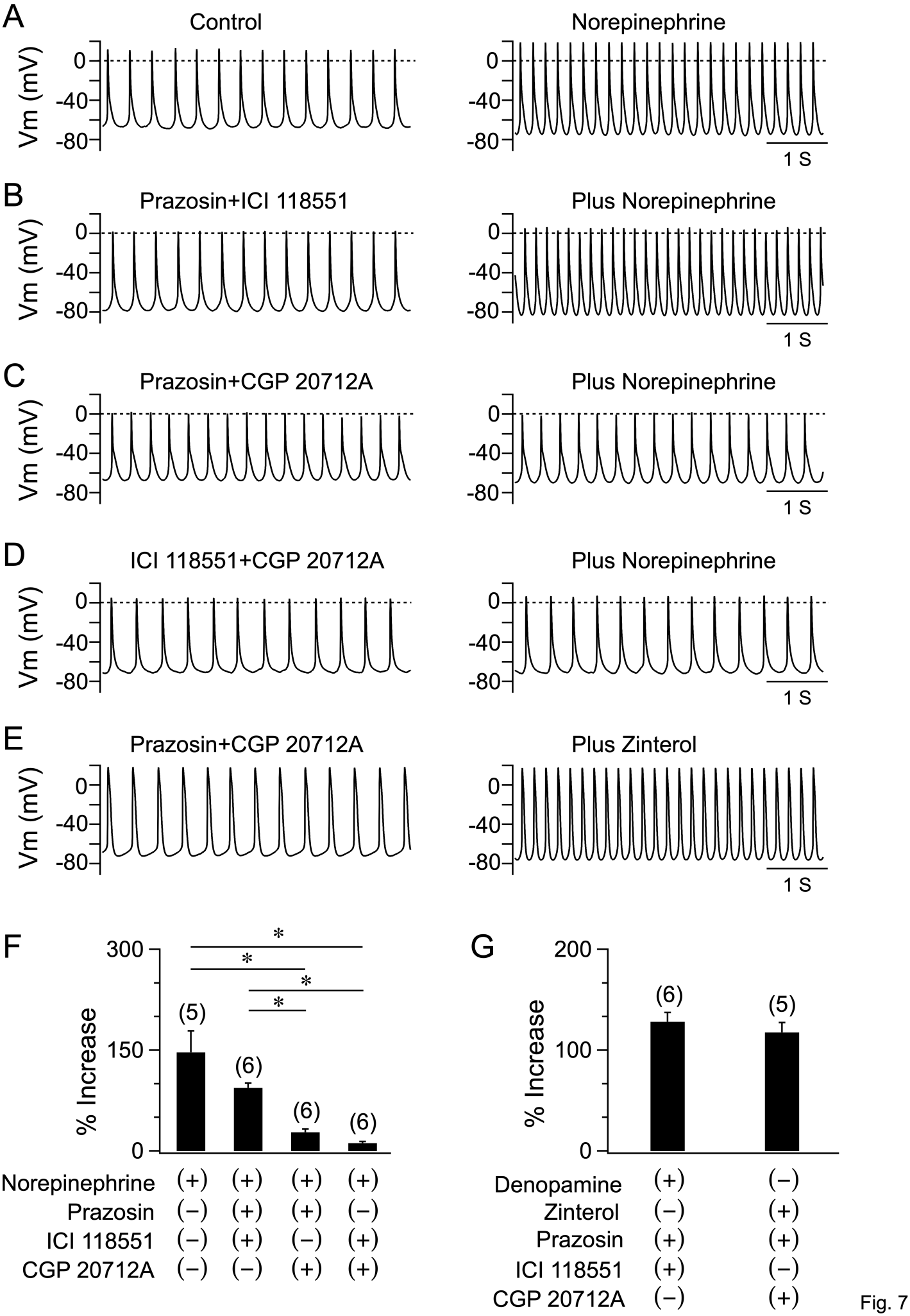
A
Control
Norepinephrine
Vm (mV)
0
-40
-80
1 S
B
Prazosin+ICI 118551
Plus Norepinephrine
C
Prazosin+CGP 20712A
Plus Norepinephrine
D
ICI 118551+CGP 20712A
Plus Norepinephrine
E
Prazosin+CGP 20712A
Plus Zinterol
F
% Increase
300
150
0
*
(5)
(6)
(6)
(6)
Norepinephrine (+) (+) (+) (+)
Prazosin (−) (+) (+) (−)
ICI 118551 (−) (+) (−) (+)
CGP 20712A (−) (−) (+) (+)
G
% Increase
200
100
0
(6)
(5)
Denopamine (+) (−)
Zinterol (−) (+)
Prazosin (+) (+)
ICI 118551 (+) (−)
CGP 20712A (−) (+)

Fig. 7

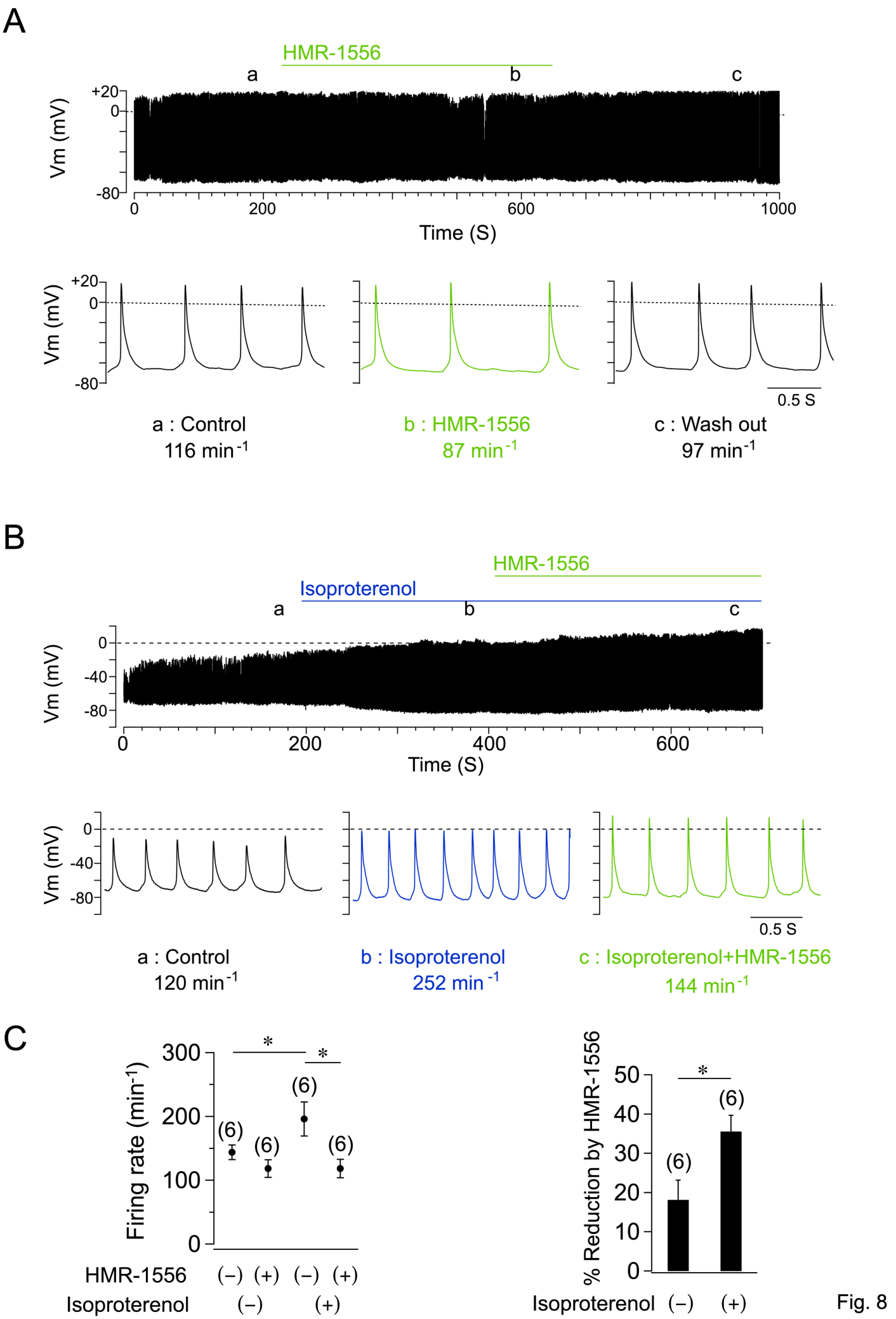
A
HMR-1556
a
b
c
Vm (mV)
+20
0
-80
0
200
600
1000
Time (S)
0.5 S
a : Control
116 min-1
b : HMR-1556
87 min-1
c : Wash out
97 min-1
B
HMR-1556
Isoproterenol
a
b
c
Vm (mV)
0
-40
-80
0
200
400
600
Time (S)
0.5 S
a : Control
120 min-1
b : Isoproterenol
252 min-1
c : Isoproterenol+HMR-1556
144 min-1
C
Firing rate (min-1)
300
200
100
0
*
*
(6)
(6)
(6)
(6)
HMR-1556 (–) (+) (–) (+)
Isoproterenol (–) (+)
% Reduction by HMR-1556
50
40
30
20
10
0
*
(6)
(6)
Isoproterenol (–) (+)

Fig. 8

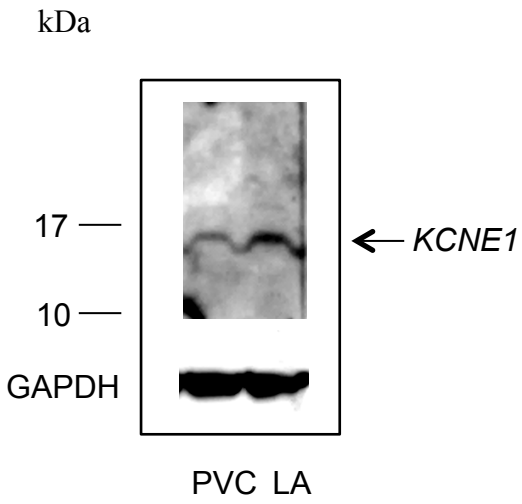

Supplementary material 1. The expression of I_{Ks} was examined using Western blotting. *KCNE1* (β-subunit) protein was detected as a signal band approximately 17 kDa in size. Note: Lysate containing protein (5 μg per lane) was separated on a 15% sodium dodecyl sulfate-polyacrylamide gel and the polyvinylidene difluoride membrane was probed with *KCNE1* APC-163 antibody (1:500 dilution in TBST; alomone labs, Israel)

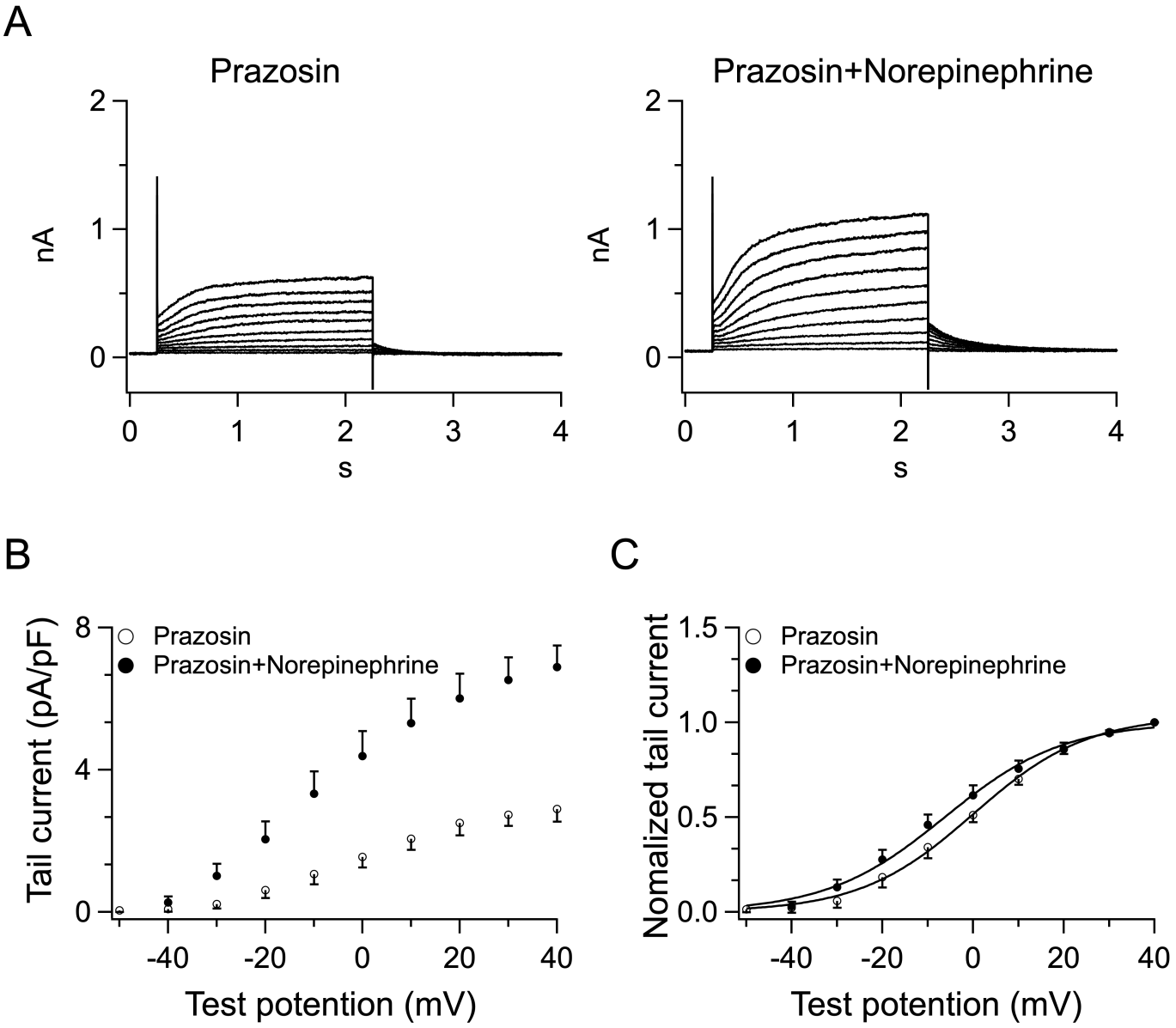

Supplementary material 2. The specific enhancement of I_{Ks} under β-adrenoceptor stimulation. (A) I_{Ks} currents recorded before and 5 min after the application of prazosin (selective α_1-adrenoceptor antagonist, 2 μM) in the absence and presence of norepinephrine (adrenoceptor agonist, 5 μM) . (B and C) Mean *I-V* relationships for the I_{Ks} tail current and the voltage dependence of I_{Ks} activation in the absence and presence of norepinephrine with prazosin hydrochloride (n = 6, N = 5; n = 6, N = 5), respectively. Data represent the mean ± S.E.M., the number of technical replicates is indicated in respective bars.